



Article

# Full-Length Transcriptome Maps of Reef-Building Coral Illuminate the Molecular Basis of Calcification, Symbiosis, and Circadian Genes

Tingyu Han <sup>1</sup>, Xin Liao <sup>2</sup>, Yunchi Zhu <sup>1</sup>, Yunqing Liu <sup>1</sup>, Na Lu <sup>1</sup>, Yixin Li <sup>1</sup>, Zhuojun Guo <sup>1</sup>, J.-Y. Chen <sup>3</sup>, Chunpeng He <sup>1,\*</sup> and Zuhong Lu <sup>1,\*</sup>

- <sup>1</sup> State Key Laboratory of Bioelectronics, School of Biological Science and Medical Engineering, Southeast University, Nanjing 210096, China  
<sup>2</sup> Guangxi Key Laboratory of Mangrove Conservation and Utilization, Guangxi Mangrove Research Center, Beihai 536000, China  
<sup>3</sup> Nanjing Institute of Paleontology and Geology, Nanjing 210008, China  
\* Correspondence: cphe@seu.edu.cn (C.H.); zhlu@seu.edu.cn (Z.L.); Tel.: +86-177-9855-0441 (C.H.); +86-186-5180-0622 (Z.L.)

**Abstract:** Coral transcriptomic data largely rely on short-read sequencing, which severely limits the understanding of coral molecular mechanisms and leaves many important biological questions unresolved. Here, we sequence the full-length transcriptomes of four common and frequently dominant reef-building corals using the PacBio Sequel II platform. We obtain information on reported gene functions, structures, and expression profiles. Among them, a comparative analysis of biomineralization-related genes provides insights into the molecular basis of coral skeletal density. The gene expression profiles of the symbiont Symbiodiniaceae are also isolated and annotated from the holobiont sequence data. Finally, a phylogenetic analysis of key circadian clock genes among 40 evolutionarily representative species indicates that there are four key members in early metazoans, including *cry* genes; *Clock* or *Npas2*; *cyc* or *Arntl*; and *tim*, while *per*, as the fifth member, occurs in Bilateria. In summary, this work provides a foundation for further work on the manipulation of skeleton production or symbiosis to promote the survival of these important organisms.

**Keywords:** reef-building corals; Symbiodiniaceae; holobionts; PacBio Sequel II; full-length transcriptome; gene expression profile; biomineralization; symbiosis; circadian clock



**Citation:** Han, T.; Liao, X.; Zhu, Y.; Liu, Y.; Lu, N.; Li, Y.; Guo, Z.; Chen, J.-Y.; He, C.; Lu, Z. Full-Length Transcriptome Maps of Reef-Building Coral Illuminate the Molecular Basis of Calcification, Symbiosis, and Circadian Genes. *Int. J. Mol. Sci.* **2022**, *23*, 11135. <https://doi.org/10.3390/ijms231911135>

Academic Editor: Tomohisa Ogawa

Received: 1 August 2022

Accepted: 19 September 2022

Published: 22 September 2022

**Publisher's Note:** MDPI stays neutral with regard to jurisdictional claims in published maps and institutional affiliations.



**Copyright:** © 2022 by the authors. Licensee MDPI, Basel, Switzerland. This article is an open access article distributed under the terms and conditions of the Creative Commons Attribution (CC BY) license (<https://creativecommons.org/licenses/by/4.0/>).

## 1. Introduction

Coral reefs are among the most productive and biodiverse ecosystems on Earth [1], and they provide survival habitats for approximately 30% of marine life [2–5]. Approximately 500 million people worldwide depend on these reefs, demonstrating their great ecological and economic value [6–10]. The scleractinian corals that mainly produce coral reefs constitute an important branch of the metazoan [2]. They show a body plan typical of Phylum Cnidaria [9] and retain many ancient gene features of ancestral metazoans [11], providing an important genetic background for studying the evolutionary origin of metazoans and bilaterians [12,13]. At present, our understanding of the molecular biology of reef-building corals largely derives from omics sequencing, and these data have provided crucial information on coral calcification [14,15], symbiosis [16–21], heat stress [22–24], acid stress [25,26], cnidocytes [27,28], collagen secretion [29], immunity [28,30–32], budding [33,34], and circadian clocks [35–37]. Despite these advances, many open questions remain.

The greatest contribution of scleractinian corals to marine biota and ecosystems is the deposition of reefs via biomineralization in calciblasts [28], which form skeletons. The reef-building coral skeleton is built through the continuous deposition of aragonite [38], which is formed by a mineral fraction consisting of calcium carbonate and an organic matrix molecule fraction that includes carbohydrates, lipids, and proteins [14]. Current reports

indicate that the main components used for calcification include calcium ATPase, carbonic anhydrase (CA), bicarbonate transporter (i.e., solute carriers 4 [SLC4] and 26 [SLC26]) and core skeleton organic matrix proteins (SOMPs) (e.g., acid-rich protein, uncharacterized skeletal organic matrix proteins [USOMPs], galaxins, and alpha IV collagen) [14,15,38–49]. However, due to the lack of full-length sequences for these genes, in-depth biological studies cannot be performed.

Phagocytosis targeting primitive algae was a prerequisite for the development of food webs involving multicellular animals [50–53]. Additionally, paleontological [51], geochemical [50,51], and molecular clock [50–52] evidence suggests that various forms of eukaryotic predation occurred during the Neoproterozoic Era (1000–541 million years ago), from the proliferation of marine algae to the origin of multicellular animal clades. At that time, increasing algal abundance created food webs with more efficient nutrient and energy transfers, driving shifts in ecosystems towards larger and increasingly complex organisms [50]. This effect is recorded in the appearance of sponges and the subsequent radiation of eumetazoans in the Ediacaran period [50]. At present, most hosts of intracellular symbionts belong to groups with polyp body plans, such as hydra, soft corals, anemones, and reef-building corals, and Mollusca, such as giant clams [16–21,27,54–56]. Among these groups, reef-building corals have particularly widespread and extensive endosymbiosis (with Symbiodiniaceae). Usually, intracellular symbiosis is thought to depend on molecular recognition for the acquisition of algae [57]. Symbiodiniaceae, similar to other dinoflagellates, must produce low doses of dinotoxins as a defense against predation or as metabolic byproducts; hence, host cells must perform certain reactions to reduce algal toxicity in an intracellular symbiotic system [58–60]. An incompatible dynamic equilibrium relationship with intracellular algae may lead to host cell death, and reducing immune rejection is a method for alleviating immune conflict and benefiting from these algae during intracellular symbioses [54]. Therefore, it is worth further exploring what the corals are obtaining by living with these algae, and whether there are differences in gene expression levels of what they supplied to different corals.

Reef-building corals show obvious circadian rhythms; interestingly, the circadian clock system and related genes have not been thoroughly investigated, although they play important roles in sustaining healthy coral growth [35–37]. Although there is a debate, which has been especially intense since 2008, on whether sponges or ctenophores are the earliest branching animals [61–68], both of them have identified some core circadian clock genes, reflecting the existence of circadian clock system in the last common animal ancestor [69–71]. At the basic molecular level, the operations of the circadian clock system and biological rhythm behavior are regulated through a conserved negative transcription-translation feedback loop, which is controlled by five key gene families [72]. Cryptochromes (CRYs) are a class of flavoproteins that can detect blue light [73]. Generally, circadian locomotor output cycles kaput (CLOCK) and its homologous protein neuronal PAS domain-containing protein 2 (NPAS2), as well as cycle (CYC) and its homologous protein brain and muscle ARNT-like (BMAL), act as positive regulatory factors, while period (PER) and timeless (TIM) act as negative regulatory factors [74]. However, the specific connections among these families vary across clades. In *Drosophila*, CRY regulates the circadian clock in a light-dependent manner [75], whereas in mice, CRY1 and CRY2 act as light-independent inhibitors of the CYC-CLOCK component [76]. However, in some invertebrates, such as monarch butterflies, CRYs exhibit both *Drosophila*-like and mammal-like functions, providing evidence of an ancestral clock gene regulation state [77,78]. Three *cry* genes and fifteen other homologous bilaterian circadian clock genes have been found in the *Acropora digitifera* coral genome [35], and 24 genes have been matched to 6 insect and 18 mammal key circadian genes via NCBI BLAST in the *Acropora millepora* coral transcriptome [36,37]. The composition and related phylogenetic pattern of circadian genes among the Anthozoa lineage remain unclear; more omics data are needed to elucidate them.

On a global scale, *Pocillopora damicornis*, *Acropora muricata*, and *Montipora foliosa* are common dominant reef-building corals in the Indo-Pacific region, and *Pocillopora verrucosa*

is a typical reef-front stony coral that protects fringing reefs [79–82]. These four corals play pivotal roles in the Indo-Pacific coral reef ecological system. Recently, increasing amounts of sequencing data derived from these reef-building corals have been deposited in public databases (see Tables 1 and S1). However, all currently available sequences have been generated using short-read (50–300 bp) sequencing approaches, leaving incomplete information and sequence splicing errors [83–85]. Critically, although some high-quality sequences have been published for both corals themselves [23,24,30–32,86–101] and their associated microorganisms [33,102–121], the reliance on short reads has prevented the precise delimitation of the gene expression profiles of reef-building corals and their endosymbiotic Symbiodiniaceae. Recent advances in long-read sequencing technology (e.g., PacBio Sequel II) have made it possible to obtain large amounts of full-length transcript data from many organisms and tissues [122–124]. In principle, such data should permit the characterization of all expressed transcripts as complete, contiguous mRNA sequences from the transcription start site to the transcription end site; in turn, this enables the more accurate and efficient analysis of the full spectrum of gene expression profile information, including data on gene expression, alternative splicing, gene fusion, expression regulation, coding sequences (CDSs), and protein structure [125–128].

**Table 1.** Sequence data of four reef-building corals in the NCBI database.

NO.	BioProject	Data Volume, Gb	Data Volume, Mbytes	Library Strategy	Platform	Model
<i>P. damicornis</i>						
1	PRJNA227785	27	17,496	RNA-Seq	Illumina	Genome Analyzer Iix
2	PRJNA299443	24	10,069	RNA-Seq	Illumina	HiSeq 4000
3	PRJNA327142	10	3750	RNA-Seq	Illumina	HiSeq 4000
4	PRJNA433950	60	23,545	RNA-Seq	Illumina	HiSeq X Ten
5	PRJNA435620	67	26,334	RNA-Seq	Illumina	HiSeq X Ten
6	PRJNA306839	18	8574	RNA-Seq	Illumina	MiSeq
7	PRJEB26650	45	21,254	RNA-Seq	Illumina	HiSeq 2500
8	<b>PRJNA544778</b>	<b>1348</b>	<b>0.41T</b>	<b>RNA-Seq</b>	<b>PacBio Illumina</b>	<b>Sequel II HiSeq X Ten</b>
9	PRJNA545379	67	27,278	RNA-Seq	Illumina	HiSeq 2000
10	PRJNA611041	258	90,416	RNA-Seq	Illumina	HiSeq 1500
<i>P. verrucosa</i>						
1	PRJNA552592	15	7782	RNA-Seq	Illumina	HiSeq 2500
2	PRJNA551401	108	47,540	RNA-Seq WGS	Illumina	HiSeq4000 HiSeq2500
3	<b>PRJNA544778</b>	<b>1348</b>	<b>0.41T</b>	<b>RNA-Seq</b>	<b>PacBio Illumina</b>	<b>Sequel III HiSeq X Ten</b>
<i>A. muricata</i>						
1	<b>PRJNA544778</b>	<b>1348</b>	<b>0.41T</b>	<b>RNA-Seq</b>	<b>PacBio Illumina</b>	<b>Sequel III HiSeq X Ten</b>
2	PRJDB8519	1785	1.09T	WGS	Illumina	HiSeq 2500
3	PRJDB5633	110	63,481	WGS	Illumina	HiSeq 2500
<i>M. foliosa</i>						
1	<b>PRJNA544778</b>	<b>1348</b>	<b>0.41T</b>	<b>RNA-Seq</b>	<b>PacBio Illumina</b>	<b>Sequel III HiSeq X Ten</b>

Only datasets of  $\geq 10$  Gb coral sequences (i.e., excluding Symbiodiniaceae sequences) are included. The bold lines indicate data generated in this paper.

To address these questions, we apply a full-length transcriptomic isoform sequencing (Iso-Seq) strategy using the PacBio Sequel II sequencing platform and quantitative gene expression analysis using the Illumina HiSeq X Ten sequencing platform to produce transcriptome maps for the four aforementioned important reef-building corals and their endosymbiotic Symbiodiniaceae. Based on the gene expression profiles, we perform a more thorough analysis of several important physiological features of reef-building corals,

including biomineralization-related gene groups, circadian gene families, and coral and Symbiodiniaceae factors related to the endosymbiotic interaction. These results enhance our understanding of the molecular biology and ecology of reef-building corals, which may aid in the recovery of marine ecosystems, and provide insights into the evolution of the circadian circuitry and holobiosis.

## 2. Results

### 2.1. Full-Length-Enriched Transcriptome Sequencing and Data Processing

Based on the standard processes of the PacBio Sequel II sequencing platform, the full-length-enriched raw transcriptome sequencing data (polymerase reads) of four coral holobionts obtained included 25.34 Gb in *P. damicornis*, 27.8 Gb in *P. verrucosa*, 22.32 Gb in *A. muricata*, and 21.44 Gb in *M. foliosa* (Tables 2 and S2). These data were filtered to ensure quality and reliability, including removing reads of less than 50 bp in length and adapter sequences (for details and statistics, see Tables 2 and S2, Figures S1 and S2). The gene expression profiles of corals and their symbiotic Symbiodiniaceae (whose transcripts were analyzed separately in a later subsection) were separated based on an alignment to previously published sequences. In terms of the corals themselves, there were 20,609 transcripts and 14,167 unigenes (N50 = 2954 bp) in *P. damicornis*, 24,174 transcripts and 12,822 unigenes (N50 = 2313 bp) in *P. verrucosa*, 31,242 transcripts and 13,800 unigenes (N50 = 2126 bp) in *A. muricata*, and 25,460 transcripts and 10,905 unigenes (N50 = 1678 bp) in *M. foliosa* (Tables 2 and S2). Unigene lengths were concentrated in the range of 1–3 kbp, with few unigenes of less than 1 kbp, verifying that the low-quality sequencing data had been filtered out (Figure S1b and Table S2.8). A previous study reported that there were 297,221 assembled transcripts (N50 = 1831 bp) and 209,337 unigenes (N50 = 1435 bp) in *P. damicornis* using a short-read sequencing approach [88]. It is obvious that PacBio sequencing can obtain fewer redundant sequences and higher-quality sequences, although we sequenced only one developmental stage of coral and not all transcripts were obtained. Then, to evaluate the level of redundancy in the data, we examined the unigene-to-transcript ratio. The percentages of unigenes with a one-to-one unigene-to-transcript ratio were 73.71% (*P. damicornis*), 64.75% (*P. verrucosa*), 57.15% (*A. muricata*), and 57.26% (*M. foliosa*), and the percentages of unigenes with a one-to-two unigene-to-transcript ratio were 17.44% (*P. damicornis*), 17.52% (*P. verrucosa*), 18.41% (*A. muricata*), and 17.18% (*M. foliosa*) (detailed in Table S2.9 and Figure S1c). The sum of the two ratios was more than 74% in all samples, indicating that data redundancy was largely reduced. Thus, we obtained high-quality full-length-enriched transcriptome sequencing data for four coral holobionts that were suitable for the subsequent analysis.

**Table 2.** Statistics of PacBio Iso-seq data.

Sample Name	<i>P. damicornis</i>	<i>P. verrucosa</i>	<i>A. muricata</i>	<i>M. foliosa</i>
Polymerase reads (Gb)	25.34	27.8	22.32	21.44
Subreads (Gb)	24.43	26.52	21.36	20.24
CCS <sup>1</sup> (Number)	334,111	292,565	341,490	305,153
FLNC <sup>2</sup> (Number)	245,504	249,577	273,822	238,498
Polished consensus (Number)	20,994	24,860	31,571	26,455
Transcripts (Number)	20,609	24,174	31,242	25,460
Unigenes (Number)	14,167	12,822	13,800	10,905
Mean length (bp)	2668	2092	1918	1472
Minimum length (bp)	51	107	183	69
Maximum length (bp)	9888	7861	6991	5942
N50 <sup>3</sup> (bp)	2954	2313	2126	1678
N90 <sup>3</sup> (bp)	1793	1346	1230	905

<sup>1</sup> CCS: circular consensus sequence. <sup>2</sup> FLNC: full-length non-chimera sequences. <sup>3</sup> N50 or 90: the length for which the collection of all subreads of that length or longer contains at least 50% or 90% of the total of the lengths of the subreads.

## 2.2. Gene-Function Annotation and Structure Analysis

To obtain comprehensive gene-function information, seven authoritative databases (NR [129], NT, Pfam [130], KOG [131], Swiss-Prot [132], KEGG [133], and GO [134]) were utilized to annotate the unigenes, and the related statistics are shown in Figure 1 (Table S3 and Figures S3–S11). In the four corals, 93.88% (*P. damicornis*), 89.32% (*P. verrucosa*), 95.10% (*A. muricata*), and 79.64% (*M. foliosa*) of the unigenes were annotated in at least one database (Figure 1a and Table S3.1). The percentage of annotated unigenes in *A. muricata*, *P. damicornis*, and *P. verrucosa* was approximately 90%, suggesting that most of the unigenes in these species were orthologues of genes with functional annotations available. In contrast, the percentage of unigenes annotated in *M. foliosa* was only 79.64% because sequencing data obtained from *Montipora* are rare, and the adaptive specialized evolution of these species means that their genomes show especially great differences from those of other reef-building corals with available omics data [100,135], limiting their in-depth annotation. It was also obvious that the percentage of annotated unigenes in *A. muricata* was higher than that in the other three corals (Figure 1b) because *A. digitifera* [136] and *A. millepora* [137], with reported genome data, both belong to the same genus as *A. muricata*, providing a good reference genome background.

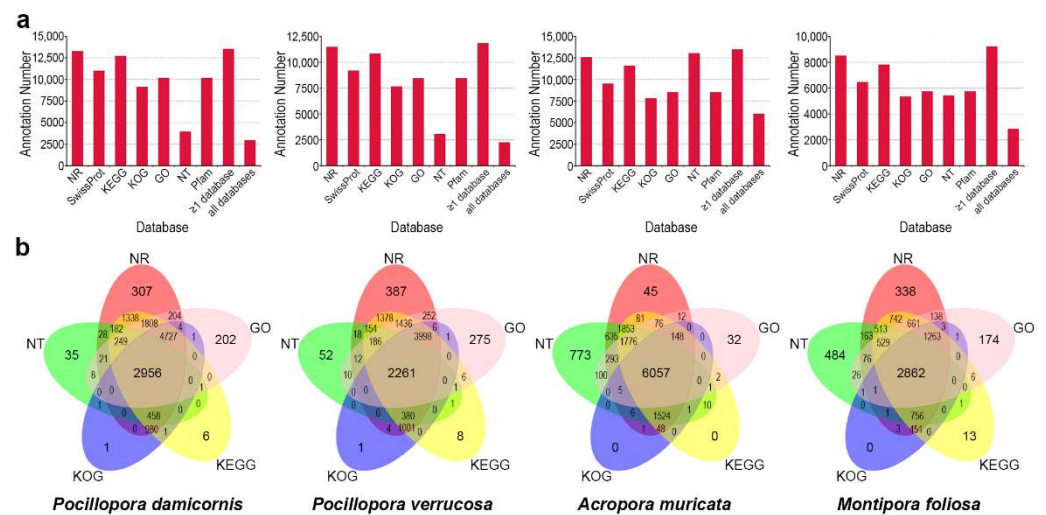


**Figure 1.** Summary of coral gene-function annotation. (a) Statistics of the annotation results of four reef-building corals, excluding Symbiodiniaceae sequences, in the NR, Swiss-Prot, KEGG, KOG, GO NT, and Pfam databases. The horizontal axis represents the different functional databases, and the vertical axis represents the number of sequences annotated in different functional databases, at least one database, and all databases. (b) Venn plots of the number of annotated sequences of four reef-building corals excluding Symbiodiniaceae sequences obtained using the NR, KEGG, KOG, GO, and NT databases. The sum of the numbers in each large circle represents the number of transcripts annotated in one database, and the overlapping circles indicate the numbers of transcripts annotated in these databases simultaneously.

To explore whether the sequences we obtained were indeed derived from cnidarians rather than from some contaminants, we counted the number of sequences annotated based on species information and observed that the top five species with the most highly similar genes to those of the four investigated corals were *A. digitifera*, *Exaiptasia pallida*, *Nematostella vectensis*, *Branchiostoma belcheri*, and *Stylophora pistillata* (or *A. millepora*) (Figure 2, Tables 3 and S3.6). These species (other than the amphioxus *B. belcheri*) are all cnidarians, and the similarities of the investigated corals to the reference species were all greater than 93%, indicating the relatively high accuracy of the annotations. Interestingly, the NR results indicate that the gene expression profiles of all four investigated corals are close to that of *B. belcheri* (Figure 2, Tables 3 and S3.6), which may be due to the slow evolution of amphioxus protein sequences.

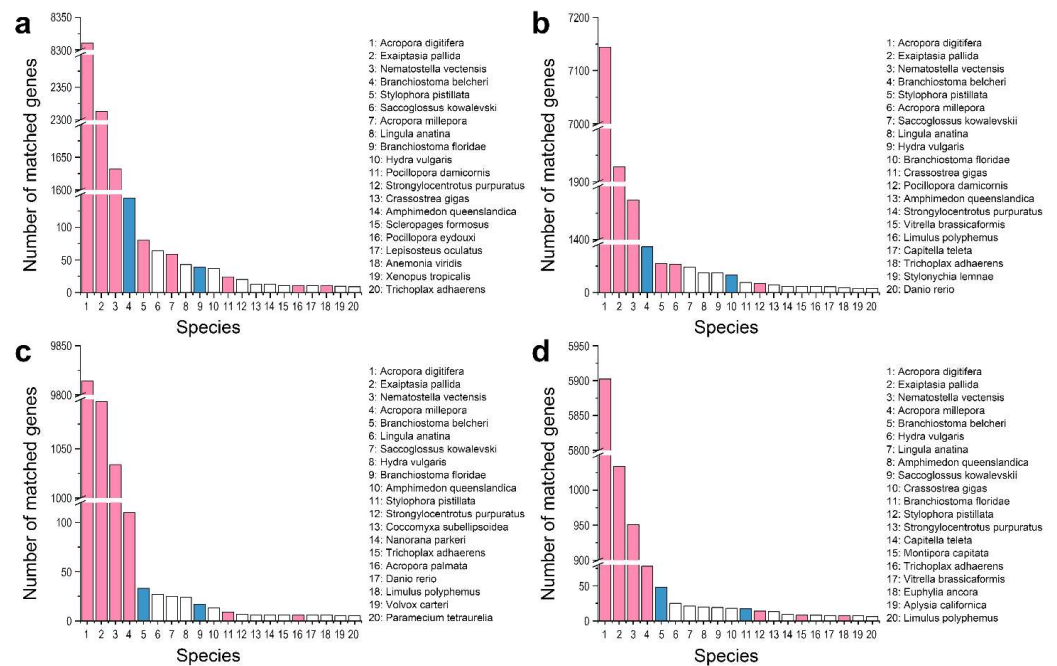


**Figure 2.** NR database annotations of corals. The top-20 species with the greatest number of top sequence hits for *P. damicornis* (a), *P. verrucosa* (b), *A. muricata* (c), and *M. foliosa* (d) are shown. The horizontal axis represents the species ID, and the vertical axis represents the number of coral unigenes annotated for different species. The pink columns represent species belonging to Anthozoa. The blue columns represent species belonging to the genus *Branchiostoma*.

**Table 3.** The top-five species with the genes most similar to the four investigated corals.

Rank	Species	Gene Number <sup>1</sup>	Percentage <sup>2</sup>
<i>P. damicornis</i>			
1	<i>Acropora digitifera</i>	8310	62.66%
2	<i>Exaiptasia pallida</i>	2313	17.44%
3	<i>Nematostella vectensis</i>	1632	12.31%
4	<i>Branchiostoma belcheri</i>	145	1.09%
5	<i>Stylophora pistillata</i>	80	0.60%
<i>P. verrucosa</i>			
1	<i>Acropora digitifera</i>	7144	62.27%
2	<i>Exaiptasia pallida</i>	1928	16.80%
3	<i>Nematostella vectensis</i>	1475	12.86%
4	<i>Branchiostoma belcheri</i>	86	0.75%
5	<i>Stylophora pistillata</i>	54	0.47%
<i>A. muricata</i>			
1	<i>Acropora digitifera</i>	9814	78.14%
2	<i>Exaiptasia pallida</i>	1098	8.74%
3	<i>Nematostella vectensis</i>	1034	8.23%
4	<i>Acropora millepora</i>	110	0.88%
5	<i>Branchiostoma belcheri</i>	33	0.26%
<i>M. foliosa</i>			
1	<i>Acropora digitifera</i>	5902	69.44%
2	<i>Exaiptasia pallida</i>	1034	12.16%
3	<i>Nematostella vectensis</i>	951	11.19%
4	<i>Acropora millepora</i>	78	0.92%
5	<i>Branchiostoma belcheri</i>	48	0.56%

<sup>1</sup> The number of coral genes that are annotated with the species listed in column 2 by NR database. <sup>2</sup> The gene number listed in column 3 as % of all in coral.

The prediction of CDSs is helpful for potential unigene analysis and provides a basis for subsequent protein analysis. The CDS lengths of the four corals were concentrated in

the range of 300–1700 nt (Materials and Methods Section and Figure S12a), and totals of 97.91% (*P. damicornis*), 95.67% (*P. verrucosa*), 95.51% (*A. muricata*), and 89.04% (*M. foliosa*) of the unigenes were predicted to contain CDS regions (Table S4.1). We then identified coral TFs among the predicted protein CDS results based on Pfam TF families (Materials and Methods Section) and found that the five largest TF families in the corals were ZBTB, zf-C2H2, homeobox, bHLH, and TF\_bZIP (Figure S12b and Table S4.2). The results of the simple sequence repeat (SSR) detection showed that most SSR sequences corresponded to poly(A) tails (Figure S12c and Table S4.3), reconfirming the absence of genomic DNA contamination. Transcripts without coding potential were classified as lncRNAs. Generally, lncRNAs were shorter than mRNAs (Figure S12e). The number of predicted lncRNAs in *M. foliosa* was much higher than those in the other corals (Figure S12d). Following CDS, TF, SSR, and lncRNA analyses, we quantified the gene expression profiles in each coral by mapping the Illumina sequencing reads to the full-length transcriptome data. This mapping directly providing read-count values that could be converted to the expected number of fragments per kilobase of transcript sequence per million base pairs sequenced (FPKM) or transcripts per kilobase million (TPM) values for further ensuring diverse quantitative analysis under different conditions (Table S5). Based on these data, the Pearson's correlation coefficient (R) analysis can be used to reflect the gene expression profile similarity among the samples, and thus verify the experimental reliability and rationality of the sample selection.

### 2.3. Gene Expression Profile Analysis

We then analyzed the gene expression profiles of the four corals (Figure 3a–d). It was clear that the gene expression levels of each coral were considered to be consistent across all replicates (Figures 3a and S13). In addition, a Pearson's  $R^2 > 0.92$  among the three biological replicates of each coral suggested that the sample selection was reasonable and the experimental data were reliable (Figure 3d). Then, the differences in the coral gene expression profiles were explored. We used two methods (median [138] and scbn [139]) to analyze the pairwise differential expressions between the two corals and showed that all six groups produced significant differential expressions of transcript orthologs ( $|\log_2\text{FoldChange}| > 2$  or 10;  $p\text{-value} < 10^{-6}$ ; see Materials and Methods Section for complete statistical analysis, Figure S14 and Table S6). Among them, the highest number of orthologous transcripts was observed between *P. damicornis* and *P. verrucosa*, while their differentially expressed genes (DEGs) accounted for the smallest proportion of all orthologous transcripts (Figure S14 and Table S6.8). Subsequently, according to the gene expression profile results, biomineralization, symbiosis, and circadian gene families, which provide crucial information on coral population structure and the evolution of coral gene repertoires, are highlighted hereafter.

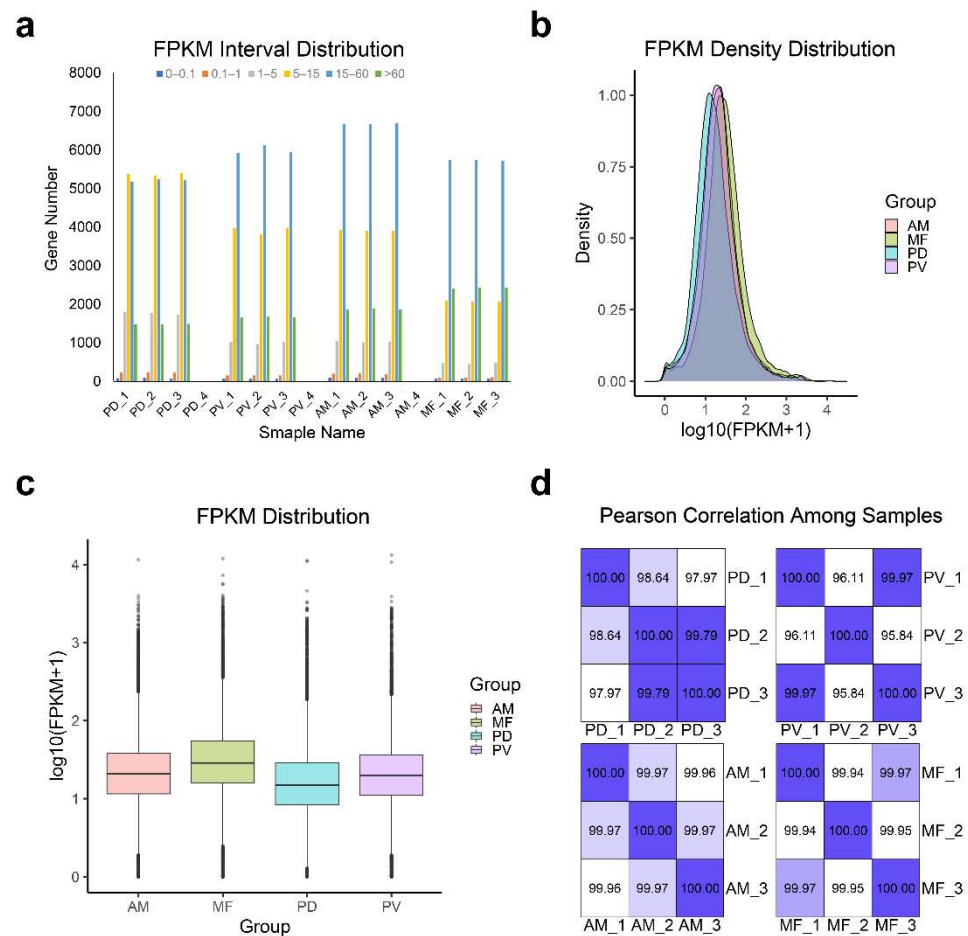


**Figure 3.** Summary of the coral gene expression level analysis. **(a)** FPKM interval distribution. The horizontal axis shows the sample name, different colors represent FPKM intervals, and the vertical axis represents the number of genes in each interval. **(b)** FPKM density distribution. The horizontal axis represents the  $\log_{10}(\text{FPKM} + 1)$  values, and the vertical axis represents the density of genes with different expression levels. **(c)** FPKM box plot. The horizontal axis shows the sample name, and the vertical axis represents the  $\log_{10}(\text{FPKM} + 1)$  values. Each box plot shows five statistical values, including the maximum, upper quartile, median, lower quartile, and minimum, from top to bottom. **(d)** Pearson's correlation among samples. The closer the value is to 1, the better the correlation. Pd: *P. damicornis*; Pv: *P. verrucosa*; Am: *A. muricata*; and Mf: *M. foliosa*.

#### 2.4. Expression Analysis of the Biomineralization-Related Gene Group

Although the biomineralization mechanisms of reef-building corals are similar (Figure 4a), they are displayed with a wide range of morphological differences. To obtain an insight into the molecular-level causes of this phenomenon, we investigated the expression patterns and features of biomineralization-related gene families and observed that the expression levels of calcium ATPases, which are essential for  $\text{Ca}^{2+}$  transport, were higher in the genera *Pocillopora* and *Acropora*, and the expression levels of bicarbonate transporters, which are essential for  $\text{HCO}_3^-$  transport, were higher in *P. verrucosa* (Figure 4b,c, Tables 4 and S7). Among the four investigated corals, *M. foliosa* had the lowest expression level of calcium ATPases, which may have a negative effect on the transportation of calcium ions to the calcifying fluid (Figure 4b, Tables 4 and S7). CA2 is universally expressed in all four corals at very high levels and accounts for a major proportion of the CA content, implying its key role in coral biomineralization (Figure 4d, Tables 4 and S7).



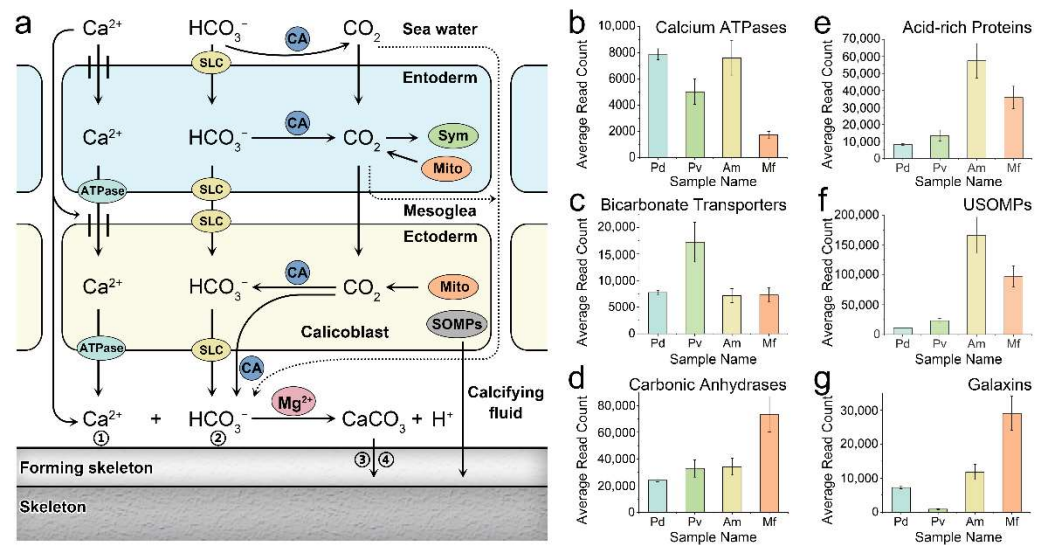


**Figure 4.** Mechanism of coral biomineralization and related gene expression levels. (a) The mechanism of reef-building coral biomineralization. (1)  $\text{Ca}^{2+}$  transport by calcium ATPase or diffusion. (2)  $\text{CO}_2$  can be converted into  $\text{HCO}_3^-$  by CA and then exits the cells via bicarbonate transporters (i.e., SLC4 and SLC26). (3) Coral acid-rich proteins and  $\text{Mg}^{2+}$  can promote crystal nucleation, determine growth axes, and control crystal growth. (4) The bioprecipitation of aragonite crystals in corals requires additional skeletal organic matrix proteins (USOMPs, galaxins, and alpha IV collagen). The average expression levels of genes belonging to calcium ATPases (b), bicarbonate transporters (c), carbonic anhydrases (d), acid-rich proteins (e), USOMPs (f), and galaxins (g). The horizontal axis shows the sample name, and the vertical axis represents the average read-count values of each set of genes. ATPase: calcium ATPase; SLC: solute carriers 4 (SLC4) and 26 (SLC26); CA: carbonic anhydrase; Sym: Symbiodiniaceae; Mito: mitochondrion; and SOMPs: coral acid-rich proteins, alpha IV collagen, galaxins, and uncharacterized skeletal organic matrix proteins (USOMPs). The solid lines represent definite paths and the dashed lines represent possible paths.

The expression levels of coral biomineralization-related extracellular matrix (ECM) proteins, including acid-rich proteins, USOMPs, galaxins, and collagen alpha-6 (VI) chain proteins, were all obviously higher in the Complexa clade (*A. muricata* and *M. foliosa*) than in the Robusta clade (*P. damicornis* and *P. verrucosa*) (Figure 4e–g, Tables 4 and S7). Regarding key acid-rich ECM proteins, *A. muricata* showed the highest expression levels, diversity, and balance, followed by *M. foliosa*, while skeletal aspartic acid-rich protein 1 (SAARP1) was the only protein in this group highly expressed in genus *Pocillopora*. Regarding the ECM accessory proteins USOMPs, *A. muricata* and *M. foliosa* presented extremely higher levels and diversity, and USOMP-6 was the dominant USOMP gene, whereas members of the genus *Pocillopora* mainly expressed USOMP-5 (Tables 4 and S7). Galaxins were the only ECM components with a higher expression in *M. foliosa* than in *A. muricata* (Tables 4 and S7). This result indicates that there are significant differences in the types and expression levels of core calcification genes among different reef-building corals, which may affect their morphological formation and growth model.

**Table 4.** Average read-count values of key biomineralization-related genes in four investigated corals.

Class	Protein Name	<i>P. damicornis</i>	<i>P. verrucosa</i>	<i>A. muricata</i>	<i>M. foliosa</i>	
Calcium ATPase	Plasma membrane calcium-transporting ATPase 1	0.00	0.00	5081.58	0.00	
	Plasma membrane calcium-transporting ATPase 2	1716.33	0.00	0.00	1171.67	
	Plasma membrane calcium-transporting ATPase 3	0.00	835.00	1049.33	528.33	
	Plasma membrane calcium-transporting ATPase 4	1596.00	1549.33	0.00	0.00	
	Plasma membrane calcium ATPase	4570.67	2626.67	0.00	0.00	
	Calcium-transporting ATPase type 2C member 1	0.00	0.00	1466.92	0.00	
	Bicarbonate Transporter	Solute carrier 4 (SLC4)	5580.66	8157.00	6321.27	5829.46
		Solute carrier 26 (SLC26)	2160.45	9072.61	850.67	1447.00
		Carbonic anhydrase 1	757.33	71.33	0.00	0.00
Carbonic anhydrase 2		22,775.35	32,853.41	31,611.00	66,451.10	
Carbonic anhydrase 3		508.33	0.00	0.00	0.00	
Carbonic anhydrase 12		0.00	0.00	2580.00	6691.27	
Acidic Proteins	Skeletal aspartic acid-rich protein 1 (SAARP1)	6423.17	11,894.42	12,233.75	3600.29	
	Skeletal aspartic acid-rich protein 2 (SAARP2)	0.00	341.41	1424.33	0.00	
	Acidic skeletal organic matrix protein (Acidic SOMP)	1831.00	1191.00	6063.00	4909.22	
	Secreted acidic protein 1 (SAP1)	0.00	0.00	0.00	5512.38	
	Secreted acidic protein 2 (SAP2)	0.00	0.00	14,584.00	8046.54	
	Aspartic and glutamic acid-rich protein	0.00	0.00	23,130.97	13,798.33	
Unique Uncharacterized Proteins	Uncharacterized skeletal organic matrix protein-1 (USOMP-1)	0.00	0.00	598.72	0.00	
	Uncharacterized skeletal organic matrix protein-2 (USOMP-2)	232.00	133.33	1202.33	4982.33	
	Uncharacterized skeletal organic matrix protein-3 (USOMP-3)	2138.94	0.00	1768.33	4098.34	
	Uncharacterized skeletal organic matrix protein-4 (USOMP-4)	0.00	0.00	21,585.00	0.00	
	Uncharacterized skeletal organic matrix protein-5 (USOMP-5)	7592.00	18,666.81	7931.45	2664.33	
	Uncharacterized skeletal organic matrix protein-6 (USOMP-6)	0.00	0.00	131,300.52	80,894.89	
	Uncharacterized skeletal organic matrix protein-7 (USOMP-7)	819.49	206.00	2158.33	4538.67	
	Uncharacterized skeletal organic matrix protein-8 (USOMP-8)	0.00	4156.33	0.00	0.00	
Galaxin	Galaxin	7224.57	862.92	6324.67	19,549.24	
	Galaxin2	0.00	0.00	5482.00	9479.72	
Collagen alpha-6(VI)	Collagen alpha-6 (VI) chain	0.00	284.67	3649.33	1082.93	

### 2.5. Genes Expressed by Symbiodiniaceae (Intracellular Symbionts of Coral) Are Mainly Involved in Energy and Nutrient Production

The secretion of calcium carbonate skeletons to form marine reefs and the reliance on intracellular symbiotic algae (Symbiodiniaceae) for nutrient acquisition are two signature features of reef-building coral physiology [14–21,136]. Although skeletal formation has been extensively discussed, the contributions of the genes expressed by the Symbiodiniaceae are rarely mentioned. Depending on identifying coral or symbiont transcripts based on alignment to previously published sequences, we found that 235 (*P. damicornis*), 351 (*P. verrucosa*), 220 (*A. muricata*), and 561 (*M. foliosa*) Symbiodiniaceae unigenes were

expressed in the investigated coral holobionts (Table S8). Similar to the analysis process used for corals, Symbiodiniaceae gene expression profiling was performed using seven functional databases, NR, NT, Pfam, KOG, Swiss-Prot, KEGG, and GO, and published Symbiodiniaceae genome data (Figures S15–S26 and Tables S8.). We found 832 transcripts that were expressed by the symbiotic Symbiodiniaceae of all four investigated corals (Figure S27), accounting for approximately 70.75% (*P. damicornis*), 70.87% (*P. verrucosa*), 88.79% (*A. muricata*), and 93.69% (*M. foliosa*) of the symbiont transcripts. Overall, gene expression profiles of the Symbiodiniaceae were more similar than those of coral hosts, suggesting considerable gene expression convergence. On the other hand, the gene expression patterns of the symbionts of *P. damicornis* and *P. verrucosa* were more similar to each other than to *A. muricata* and *M. foliosa*, and vice versa, coinciding with the evolutionary relationships of the corals (Figure S28).

To explore the functions of these expressed genes, we classified them according to the annotation results using the GO database (Figures 5 and S29, and Tables S8.11 and S8.12). In the biological process category, the identified gene functions were mainly involved in oxidation reduction and carbohydrate metabolism (Figure 5). In the cellular component category, most of the functional genes were related to photosynthesis, such as light-harvesting complex or photosystem (Figure S29). In the molecular function category, the largest group of genes was associated with oxidoreductase or carbonate dehydratase activity (Figure S29). These results suggest that the symbionts of all four corals have similar expression profiles that feature genes related to energy and nutrient production.

## 2.6. Phylogenetic Analysis of the Key Circadian Clock Gene Regulation Network

The circadian clock system is one of the most universal and fundamental characteristics of life across almost all living species [74]. Corals also exhibit circadian behaviors, and there have been studies describing the molecular mechanisms underlying the regulation of these behaviors [35–37]. However, whether this mechanism is applicable to other corals, other cnidarians and even other animals remains to be clarified. To explore the evolutionary origins of the key members of the circadian clock gene regulation network of reef-building corals, including the four corals studied herein, we selected 40 evolutionarily representative species and used their protein models to investigate the key circadian clock gene regulation network, namely, the *cry1*, *cry2*, *Clock*, *Npas2*, *cyc*, *Arntl* (also known as *Bmal1*), *Arntl2* (also known as *Bmal2*), *per1*, *per2*, *per3*, and *tim* genes (Tables 5 and S9), and performed phylogenetic analyses (Figures 6 and S30–S38). The results show that the key circadian clock gene regulatory network evolves in early metazoans, whereas protozoan clade does not have this kind of gene regulatory network, although the *tim* orthologous gene is found in the Ciliophora clade. Moreover, the Ascidiacea clade showed a complete loss of this network during evolutionary adaptation, except for the *tim* gene, suggesting that ascidians might have unknown clock mechanisms that differ from known systems of vertebrates and insects (Tables 5 and S9, Figures 6 and S30–S38). Among this group of genes, the *tim* gene was the only one present in all the searched species, suggesting that it is the most conserved and stable circadian clock gene (Tables 5 and S9, Figure 6) [100,140]. The phylogenetic analysis suggested that in the early metazoan stage (non-bilaterian metazoans), there were four key gene members of the circadian clock gene regulatory network, *cry*; *Clock* or *Npas2*; *cyc*, *Arntl*(*Bmal1*), or *Arntl2*(*Bmal2*); and *tim*. The *cry*, *Clock* or *Npas2*, *cyc* or *Arntl* (*Bmal1*), and *tim* gene homologues can be found in reef-building corals as shown in Table 5. Thus, the data suggested the existence of four key conserved members of the reef-building coral circadian clock gene regulation network. The phylogenetic analysis also indicated that the *per* gene is a novel member of the circadian clock gene regulation network in the Bilateria, as it is found in protostomes and deuterostomes but not in early metazoans (Table 5).

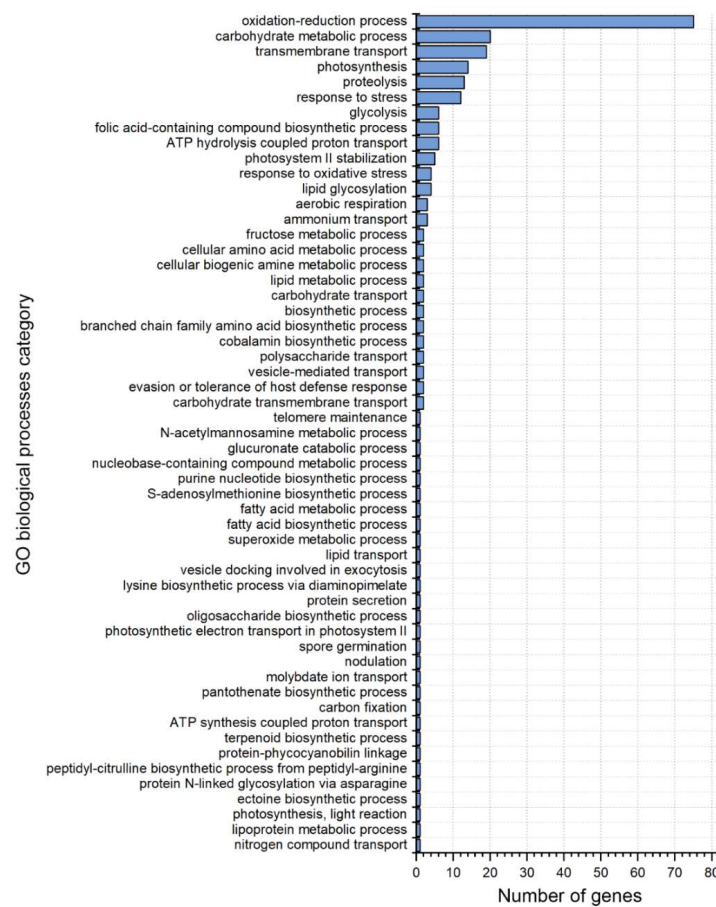


**Figure 5.** Bar graph of co-expressed Symbiodiniaceae sequences based on GO biological processes categories. The vertical axis represents the GO terms, and the horizontal axis represents the number of transcripts annotated to the terms (including sub-terms of the terms).

**Table 5.** Presence of key circadian clock gene homologues in representative species.

Lineage	Key Circadian Clock Genes										
	<i>cry1</i>	<i>cry2</i>	<i>Clock</i>	<i>Npas2</i>	<i>cyc</i>	<i>Arntl</i> ( <i>Bmal1</i> )	<i>Arntl2</i> ( <i>Bmal2</i> )	<i>per1</i>	<i>per2</i>	<i>per3</i>	<i>tim</i>
Mammalia	Y	Y	Y	Y	-	Y	Y	Y	Y	Y	Y
Actinopterygii	Y	Y	Y	Y	-	Y	Y	Y	Y	Y	Y
Ascidiacea	-	-	-	-	-	Y	-	-	-	-	Y
Cephalochordata	Y	-	-	Y	-	Y	-	Y	-	-	Y
Echinoidea	Y	Y	Y	-	-	Y	-	-	-	-	Y
Enteropneusta	-	-	Y	-	-	Y	-	-	-	-	Y
Nematoda	-	-	-	-	-	Y	-	-	-	-	Y
Insecta	Y	-	Y	-	Y	-	-	Y	-	-	Y
Bivalvia	Y	-	Y	-	Y	-	-	Y	-	-	Y
Platyhelminthes	-	-	-	-	-	Y	-	-	-	-	Y
Anthozoa	Y	Y	Y	Y	Y	Y	-	-	-	-	Y
Hydrozoa	Y	-	-	-	-	Y	-	-	-	-	Y
Cubozoa	-	-	-	Y	-	Y	-	-	-	-	Y
Scyphozoa	Y	-	-	-	-	Y	-	-	-	-	Y
Porifera	-	Y	Y	-	Y	-	-	-	-	-	Y
Ctenophora	Y	-	Y	-	-	Y	-	-	-	-	Y
Ciliophora	-	-	-	-	-	-	-	-	-	-	Y

“Y” means yes, which means the species contains this gene homologue, while “-” means the opposite.

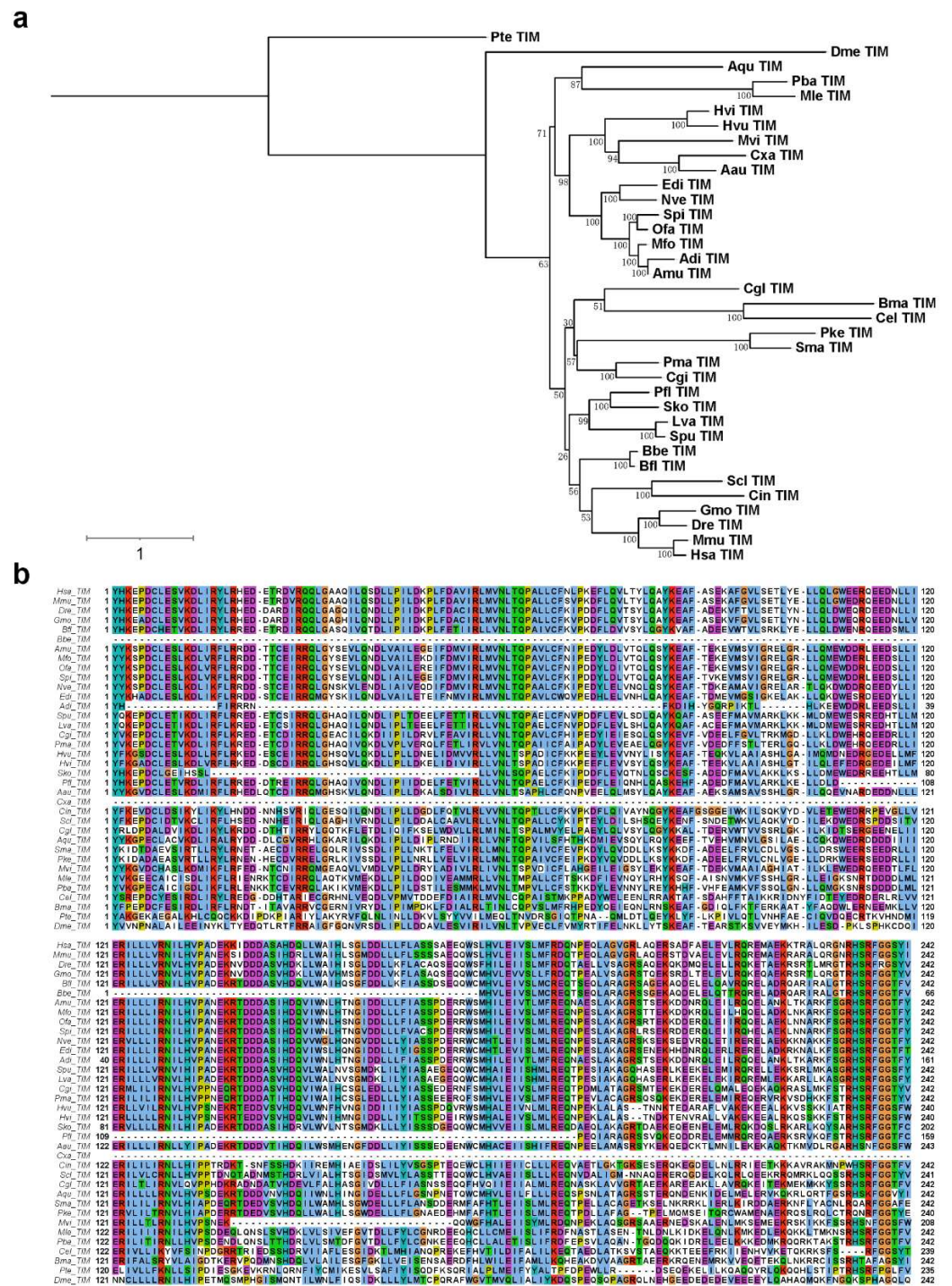


**Figure 6.** *Tim* gene phylogenetic analysis. (a) Phylogenetic tree of *tim* genes based on the maximum likelihood method with best-fit model selection. Branch lengths are optimized by maximum likelihood on original alignment and the numbers are bootstrap supports (%). (b) Partial conserved domain (pfam04821) of *tim* genes among different species. The complete conserved domain is shown in Figure S38.

### 3. Discussion

Despite much research, our understanding of reef-building coral holobiont transcriptomes remains incomplete, and the short-read lengths intrinsic to the prevailing technologies have limited access to complete genetic information. Here, we were sequenced and analyzed the full-length transcriptomes of four common dominant reef-building coral holobionts with respect to gene functions, structures, and expression. The results reveal differences in

the members actually involved in biomineralization processes in reef-building corals and provide new insights into further understanding the molecular mechanisms of coral density. In particular, we isolated and demarcated the gene expression profiles of the symbiont Symbiodiniaceae, which showed a higher convergence than the coral hosts, suggesting that the internal environment of symbiotic algae-bearing cells in all four species may be quite similar. Moreover, we confirmed that there were four key members of the circadian clock gene regulatory network in early metazoans and that the *per* gene first occurred in Bilateria, further enriching the molecular database for studying the evolutionary origins of the animal circadian clock system, although this needs to be verified by biological experiments or other methods.

### 3.1. Coral Biomineralization and Skeleton Density

Coral biomineralization has been intensively studied in previous studies, but descriptions of its formation mechanism vary; here, we summarized this process, which consists of four components (Figure 4a). (1) Calcium ion transport. In calcicoblasts and paracells, calcium ions enter the cells through calcium channels and exit via calcium ATPases that exchange two calcium ions for four protons across the cell membrane [39,40].  $\text{Ca}^{2+}$  diffusion among cells with chemical gradients may also participate in calcium deposition [15]. (2) An  $\text{HCO}_3^-$  source. The source of  $\text{HCO}_3^-$  is metabolic and environmental  $\text{CO}_2$ . Metabolic  $\text{CO}_2$  can be converted into  $\text{HCO}_3^-$  both intracellularly and extracellularly, which is catalyzed by CA under a favorable pH [41–43], and intracellular  $\text{HCO}_3^-$  exits cells via bicarbonate transporters belonging to two membrane protein families (SLC4 and SLC26) [44]. In calcifying fluid, the  $\text{HCO}_3^-$  concentration is higher than the  $\text{Ca}^{2+}$  concentration, and the amount of calcium carbonate deposition is determined by the  $\text{Ca}^{2+}$  concentration [43]. (3) Acid-rich proteins. Coral acid-rich proteins are key ECM proteins involved in biomineralization and can interact with amorphous calcium carbonate (ACC) directly, promoting crystal nucleation, determining growth axes and controlling crystal growth [45,46]. (4) Other organic matrix proteins of the ECM. The bioprecipitation of aragonite crystals in corals also requires additional skeletal organic matrix proteins as binders [47], including USOMPs, galaxins, and alpha IV collagen [38,48,49]. In addition, magnesium plays a crucial role in regulating the formation of different calcium carbonate phases that cooperate with organic matrix molecules to stabilize ACCs [141].

Here, the above core biomineralization-related gene expression level analyses among four reef-building corals indicate that the genera *Pocillopora* and *Acropora* may have a greater capacity to produce calcium carbonate than the genus *Montipora*, but the opposite situation was observed for biomineralization-related ECM proteins from the genus *Pocillopora*, suggesting that the species of the Complexa clade may produce a greater volume of skeleton than those of the Robusta clade using the same amount of calcium carbonate. This is in accordance with the reported skeletal density data of these stony corals [34,142]; however, future studies on the relationship between the activity and stability of biomineralization-related enzymes among different corals at the protein level are required to confirm this conjecture.

### 3.2. Evolutionary Origins of the *per* Gene

The oscillations of both the transcript and protein levels of the *per* gene have a period of approximately 24 h and play a central role in the molecular mechanism of the biological clock driving circadian rhythms. In *Drosophila*, after PER is produced from *per* mRNA, it dimerizes with timeless (TIM), and the complex enters the nucleus and inhibits the TFs *per* and *tim*, which in turn lowers the levels of PER and TIM [53]. When TIM is not complexed with PER, another protein, double-time, or DBT, phosphorylates PER, targeting it for degradation [57]. In mammals, an analogous transcription-translation negative feedback loop is observed. One of the three PER proteins (PER1, PER2, and PER3) that is translated from the mammalian homologs of drosophila-*per* dimerizes via its PAS domain with one of two cryptochrome proteins (CRY1 and CRY2) to form a negative element of the clock. This

dimer then interacts with the CLOCK (or NPAS2) and ARNTL (or ARNTL2) heterodimer, inhibiting its activity and thereby negatively regulating its own expression [143]. Despite an extensive search, we failed to detect orthologs of the *per* gene in our coral data. This also may be the case for sponges and ctenophores (Tables 5 and S9). On the other hand, amphioxus [144,145] and *Crassostrea gigas* [146] likely have *per* genes, and our results show that the biological clock is a common feature of a wide range of Metazoa, while *per* gene originates from Bilateria. It is unclear, however, whether the ancient circadian clock system initially operated without the *per* gene, whether the non-bilaterian metazoans system lost this locus via deletion or other mutation, or whether unknown proteins may have functions similar to the *per* gene. These hypotheses need to be explored further in future research.

Overall, the full-length transcriptome maps of reef-building coral may serve as references for expression analyses of coral under environmental stressors linked to global change, which alter the normal function of reef-building corals. As long-read sequencing continues to evolve in throughput, accuracy, accessibility, and cost efficiency, full-length transcriptomes will be adopted by researchers and provide us with unprecedented views of serious biological problems. However, genome, small RNA, proteome, and single-cell data are still lacking to further understand the biology of reef-building corals. Future efforts are required to construct a coral genome database as a reference for analyzing functional genes and their associated regulatory networks at the transcriptomic and proteomic levels and further refine them to specific cellular lineages.

## 4. Materials and Methods

### 4.1. Ethics

All coral samples were collected and processed in accordance with local laws for invertebrate protection.

### 4.2. Sample Collection

The corals in the study were collected from the Xisha Islands in the South China Sea (latitude 15°40'–17°10' N, longitude 111°–113° E).

### 4.3. Coral Culture System

The coral samples were cultured in our laboratory coral tank with conditions conforming to their habitat environment. All samples were raised in a RedSea® tank (redsea575, Red Sea Aquatics Ltd., London, UK) at 26 °C and 1.025 salinity (Red Sea Aquatics Ltd., London, UK). The physical conditions of the coral culture system were as follows: three coral lamps (AI®, Red Sea Aquatics Ltd., London, UK), a protein skimmer (Reef Octopus Regal 250-S, Honya Co. Ltd., Shenzhen, China), a water chiller (tk1000, TECO Ltd., Port Louis, Mauritius), two wave devices (VorTech™ MP40, EcoTech Marine Ltd., Bethlehem, PA, USA), and a calcium reactor (Reef Octopus OCTO CalReact 200, Honya Co. Ltd., Shenzhen, China).

### 4.4. Total RNA Extraction

The three biological replicates samples for each coral were isolated from three healthy branches in the same coral independent colony to ensure that enough high-quality RNA (>15 µg) could be obtained for a PacBio cDNA library and three Illumina cDNA libraries. All the RNA extraction procedures followed the manufacturer's instructions. The total RNA was isolated with TRIzol® LS Reagent (Thermo Fisher Scientific, 10296028, Waltham, MA, USA) and treated with DNase I (Thermo Fisher Scientific, 18068015, Waltham, MA, USA). The high-quality mRNA was isolated with a FastTrack MAG Maxi mRNA Isolation Kit (Thermo Fisher Scientific, K1580-02, Waltham, MA, USA). The RNA extraction procedure was performed according to the following instructions: (1) grinded coral samples (kept the samples submerged in liquid nitrogen at all times); (2) when the samples were ground into small pieces, the TRIzol® LS reagent was added, the ratio of sample to reagent was about 1:3; (3) we let samples stand and thaw naturally; (4) we continued adding TRIzol®

LS reagent until the samples were dissolved, and dispensed into 50 mL centrifuge tubes; (5) centrifuged at 4 °C and 3000 rpm for 5–15 min; (6) dispensed the supernatant into 50 mL centrifuge tubes; (7) added BCP (Molecular Research Center, BP 151, Cincinnati, OH, USA) to the above centrifuge tubes, the ratio of sample to reagent was about 5:1, shaken well and then stood for 10 min; (8) centrifuged at 4 °C and 10,500 rpm for 15 min; (9) we obtained the supernatant, added an equal volume of Isopropanol (Amresco, 0918-500ML, Radnor, PA, USA) and mixed well, stood them overnight at –20 °C; (10) centrifuged at 4 °C and 10,500 rpm for 30 min, discarded the supernatant; and (11) rinsed them 2 times with 75% Ice Ethyl alcohol, Pure (Sigma-Aldrich, E7023-500ML, Taufkirchen, München, Germany). Finally, three samples of each coral were extracted in equal amounts (total >10 µg) and mixed for PacBio full-length-enriched transcriptome sequencing; the remainders (>1.5 µg per sample) were used for Illumina sequencing.

#### 4.5. Total RNA Quality Testing

Before establishing the library, the quality of total RNA must be tested. RNA degradation and contamination were monitored on 1% agarose gels electrophoresis; RNA purity (OD<sub>260</sub>/280 ratio) was checked using the NanoPhotometer<sup>®</sup> spectrophotometer (IMPLEN, Westlake Village, CA, USA); RNA concentration was quantified using Qubit<sup>®</sup> RNA Assay Kit in Qubit<sup>®</sup> 2.0 Fluorometer (Thermo Fisher Scientific, Waltham, MA, USA); and RNA integrity was assessed using the RNA Nano 6000 Assay Kit of the Agilent Bioanalyzer 2100 system (Agilent Technologies, Santa Clara, CA, USA).

#### 4.6. Illumina cDNA Library Construction and Sequencing

A total amount of 1.5 µg RNA per sample was used as input material for the RNA sample preparations. Sequencing libraries were generated using NEBNext<sup>®</sup> Ultra<sup>™</sup> RNA Library Prep Kit (E7530L) for Illumina<sup>®</sup> (NEB, Ipswich, MA, USA) following the manufacturer's recommendations, and index codes were added to attribute sequences to each sample. Briefly, mRNA was purified from total RNA using poly-T oligo-attached magnetic beads. Fragmentation was performed using divalent cations under an elevated temperature in NEBNext First-Strand Synthesis Reaction Buffer (5×). First-strand cDNA was synthesized using a random hexamer primer and M-MuLV Reverse Transcriptase (RNase H<sup>-</sup>). Second-strand cDNA synthesis was subsequently performed using DNA Polymerase I and RNase H. Remaining overhangs were converted into blunt ends via exonuclease/polymerase activities. After adenylation of 3' ends of DNA fragments, an NEBNext Adaptor with hairpin loop structure was ligated to prepare for hybridization. In order to select cDNA fragments preferentially 250–300 bp in length, the library fragments were purified with an AMPure XP system (Beckman Coulter, Beverly, Brea, CA, USA). Then, 3 µL USER Enzyme (NEB, Ipswich, MA, USA) was used with size-selected, adaptor-ligated cDNA at 37 °C for 15 min followed by 5 min at 95 °C before PCR. Then, PCR was performed with Phusion High-Fidelity DNA polymerase, Universal PCR primers, and Index (X) Primer. Finally, PCR products were purified (AMPure XP system) and library quality was assessed on the Agilent Bioanalyzer 2100 system. The clustering of the index-coded samples was performed on a cBot Cluster Generation System using TruSeq PE Cluster Kit v3-cBot-HS (Illumina, San Diego, CA, USA), according to the manufacturer's instructions. After cluster generation, the library preparations were sequenced on an Illumina HiSeq X Ten platform and paired-end reads were generated.

#### 4.7. PacBio cDNA Library Construction and Sequencing

The isoform sequencing (Iso-Seq) library was prepared according to the isoform sequencing protocol (Iso-Seq) using the Clontech SMARTer<sup>®</sup> PCR cDNA Synthesis Kit (Clontech Laboratories (now Takara Laboratories), 634926, Mountain View, CA, USA) and the BluePippin Size Selection System protocol, as described by Pacific Biosciences (PN 100-092-800-03). Briefly, Oligo(dT)-enriched mRNA was reversely transcribed to cDNA by a SMARTer PCR cDNA Synthesis Kit; the synthesized cDNA was then amplified by



polymerase chain reaction (PCR) using BluePippin Size-Selection System protocol; the Iso-Seq library was constructed by full-length cDNA damage repair, terminal repair, and attaching SMRT dumbbell adapters; the sequences of the unattached adapters at both ends of the cDNA were removed by exonuclease digestion; the cDNA obtained above was combined with primers and DNA polymerase to form a complete SMRT bell library. While the library was qualified, the PacBio Sequel II platform was used for sequencing based on the effective concentration and data output requirements of the library.

#### 4.8. Data Filtering and Processing

The Illumina sequencing raw reads of fastq format were firstly processed through in-house perl scripts. In this step, clean data were obtained by removing reads containing adapters, reads containing ploy-N, and low-quality reads from raw data. At the same time, Q20, Q30, GC-content, and sequence duplication levels of the clean data were calculated. All the downstream analyses were based on clean data with a high quality.

The PacBio sequencing raw data were processed by SMRTlink v8.0 (Pacbio, Menlo Park, CA, USA) software. The circular consensus sequence (CCS) was generated from sub-read BAM files with the following parameters: min\_length 50, min\_passes 1, max\_length 15,000. CCS.BAM files were output, which were then classified into full-length and non-full-length reads using lima, removing polyA using refine. Full-length fasta files produced were then fed into the cluster step, which performed isoform-level hierarchical clustering ( $n \times \log(n)$ ), followed by final arrow polishing, hq\_quiver\_min\_accuracy 0.99, bin\_by\_primer false, bin\_size\_kb 1, qv\_trim\_5p 100, and qv\_trim\_3p 30.

#### 4.9. Coral and Symbiodiniaceae Sequences Separation

We aligned consensus reads to coral or Symbiodiniaceae reference genomes, respectively, using GMAP v2017-06-20 (Thomas D. Wu, South San Francisco, CA, USA) software [147]. The sequences mapped to Symbiodiniaceae reference genomes belonged to Symbiodiniaceae sequences; the sequences mapped to coral reference genomes belonged to coral sequences.

#### 4.10. Correction and De-Redundancy

The RNA-seq data sequenced by the Illumina HiSeq X Ten platform were used to correct additional nucleotide errors in polish consensus sequences obtained in the previous step with LoRDEC v0.7 (Leena Salmela and Eric Rivals, Helsinki, Finland) software [148]. Using CD-HIT v4.6.8 (Weizhong Li, La Jolla, CA, USA) software (parameters:  $-c$  0.95  $-T$  6  $-G$  0  $-aL$  0.00  $-aS$  0.99), all redundancies were removed in corrected consensus reads to acquire final full-length transcripts and unigenes for subsequent bioinformatics analysis [149].

#### 4.11. Gene-Function Annotation

Gene functions were annotated using the following databases: NT (NCBI non-redundant nucleotide sequences); NR (NCBI non-redundant protein sequences); Pfam (protein family); KOG/COG database (clusters of orthologous groups of proteins); Swiss-Prot (a manually annotated and reviewed protein sequence database); KEGG (Kyoto Encyclopedia of Genes and Genomes); and GO (gene ontology). We used BLAST 2.7.1+ (Christiam Camacho, Bethesda, MD, USA) software [150] with the e-value  $1 \times 10^{-5}$  for NT database analysis, Diamond v0.8.36 (Benjamin Buchfink, Tübingen, Germany) BLASTX software [151] with the e-value  $1 \times 10^{-5}$  for NR, KOG, Swiss-Prot and KEGG databases analyses, and HMMER 3.1 (Sean R. Eddy, Ashburn, VA, USA) package [152] for Pfam database analysis.

#### 4.12. Gene Structure Analysis

ANGEL v2.4 (Kana Shimizu, Tokyo, Japan) software [153] was used to predict protein CDS (coding sequence). We used same species or closely related species confident protein sequences for ANGEL training and then ran the ANGEL prediction for the given sequences.

Usually, the TFs were identified based on the Pfam files of TF families in the AnimalTFDB 3.0 database [154]; however, corals were not included in this database, so we identified coral TFs based on the Pfam files of TF families using the hmmsearch program in HMMER 3.1 package. SSR of the transcriptomes was identified using MISA v1 (Thomas Thiel, Gatersleben, Germany) [155]. We used CNCI v2 (Liang Sun, Beijing, China) [156], CPC2 v0.1 (Yu-Jian Kang, Beijing, China) [157], PfamScan v1.6 (EMBL-EBI, Cambridgeshire, UK) [158], and PLEK v1.2 (Aimin Li and Junying Zhang, Xi'an, China) [159], four tools to predict the coding potential of transcripts. Transcripts predicted with coding potential by either/all of the three tools above were filtered out, and those lacking coding potential were our candidate set of lncRNAs.

#### 4.13. Gene Expression Quantification

The full-length transcriptomes of each coral obtained above were used as the reference backgrounds, respectively, and then the clean reads for the corresponding three biological replicate samples obtained by Illumina sequencing were mapped to it and the read-count values for each transcript can be obtained by kallisto v0.44.0 (Pachter Lab, Berkeley, CA, USA) software [160]. The read counts were converted to FPKM to analyze the gene expression levels. Using Pearson's correlation coefficient, we analyzed the relationship among the samples.

#### 4.14. Gene Differential Expression Analysis

Based on the above steps, we obtained gene expression levels for a total of 12 samples from 4 coral species (Table S5.1). Orthologous transcripts between each of the two corals were searched by orthofinder v2.5.4 (David M. Emms, Oxford, UK) [161]. To make the expression levels of orthologous genes comparable between different species, we used two methods (median [138] and scbn [139]) to normalize their expression levels. Both of them were based on a group of conserved orthologous genes among different species. Therefore, we selected orthologous transcripts that were uniquely present in all four coral species as conserved orthologous genes. Then, we used the median method by assessing their median expression levels in each species among the genes with expression values in the interquartile range for different species and deriving the scaling factor that adjusted those median values to a common value. Meanwhile, we used these conserved orthologous genes by minimizing the deviation between the empirical and nominal type-I errors to achieve the optimal scaling factor in the scbn method. Accordingly, the normalized expression matrix and the  $p$ -value of each pair of orthologous transcripts can be obtained. Orthologous transcripts with  $p$ -value  $< 10^{-6}$  and  $|\log_2(\text{FoldChange})| > 2$  or 10 were regarded as DEGs.

#### 4.15. Phylogenetic Analysis

To construct the phylogenetic tree, 4 of our own reef-building corals and 36 other species were selected for the study, for a total of 17 clades, with the exception of the Porifera clade for which no further protein model species could be found; 2 two or more representative species per clade were selected to reduce the contingency of results (Table 5 and detailed in Table S9). The confirmed amino acid sequences of circadian clock genes of *Homo sapiens*, *Mus musculus*, *Danio rerio*, and *Drosophila melanogaster* were used as query sequences to search for orthologs in the protein models of the above species using the BLASTp algorithm at the local BLAST+ 2.13.0 (parameters:  $e$  value =  $1 \times 10^{-5}$ ). The sequences alignment was performed using MAFFT v7.505 (Kazutaka Katoh, Tokyo, Japan) with default parameters [162]. The gaps were removed to obtain conserved domains by trimAl v1.4.rev15 (Salvador Capella-Gutiérrez, Barcelona, Spain) with default parameters [163]. The phylogenetic trees were constructed using the maximum likelihood method by IQ-TREE 2.0.7 (Bui Quang Minh, Canberra, ACT, Australia) with the parameters:  $-m$  MFP  $-B$  1000  $-alrt$  1000 (" $-m$  MFP" means that it can automatically determine the best-fit model for data, " $-B$  1000" specifies 1000 replicates for the ultrafast bootstrap, and " $-alrt$  1000" specifies the number of bootstrap replicates for SH-aLRT where 1000 is the minimum

number recommended) [164–166]. iTOL v6.3.2 (Ivica Letunic, Heidelberg, Germany) [167] was used to visualize the tree and Jalview 2.11.2.4 (Andrew M. Waterhouse, Cambridge, MA, USA) was used to show the conserved domains [168]. The names (abbreviations) of the 40 species were as follows: *H. sapiens* (Hsa), *M. musculus* (Mmu), *D. rerio* (Dre), *Gadus morhua* (Gmo), *Ciona intestinalis* (Cin), *Styela clava* (Scl), *B. floridae* (Bfl), *B. belcheri* (Bbe), *Strongylocentrotus purpuratus* (Spu), *Lytechinus variegatus* (Lva), *Saccoglossus kowalevskii* (Sko), *Ptychodera flava* (Pfl), *Caenorhabditis elegans* (Cel), *Brugia malayi* (Bma), *D. melanogaster* (Dme), *Cotesia glomerata* (Cgl), *C. gigas* (Cgi), *Pecten maximus* (Pma), *Schistosoma mansoni* (Sma), *Paragonimus kellicotti* (Pke), *P. damicornis* (Pda), *P. verrucosa* (Pve), *A. muricata* (Amu), *M. foliosa* (Mfo), *A. digitifera* (Adi), *S. pistillata* (Spi), *Orbicella faveolata* (Ofa), *N. vectensis* (Nve), *E. diaphana* (Edi), *Hydra vulgaris* (Hvu), *Hydra viridissima* (Hvi), *Morbakka virulenta* (Mvi), *Alatina alata* (Aal), *Aurelia aurita* (Aau), *Cassiopea xamachana* (Cxa), *Amphimedon queenslandica* (Aqu), *Mnemiopsis leidyi* (Mle), *Pleurobrachia bachei* (Pba), *Paramecium tetraurelia* (Pte), and *Ichthyophthirius multifiliis* (Imu).

## 5. Conclusions

The sequencing and analysis of the full-length transcriptome maps of dominant reef-building coral holobionts contributed to a more in-depth understanding of coral physiology. Related insights improve our understanding of the evolution of circadian rhythms and of holobiosis, and they provide a foundation for further work to protect or even manipulate coral skeleton production or symbiosis to promote the survival of these important organisms. These results provide support for remodeling reef-building corals through advanced gene toolkits under current global climate change and ecological deterioration.

**Supplementary Materials:** The supporting information can be downloaded at: <https://www.mdpi.com/article/10.3390/ijms231911135/s1>.

**Author Contributions:** Experiment, data analysis, writing, and editing, T.H.; conceptualization, project administration, and reviewing, C.H.; supervision, Z.L. and J.-Y.C.; funding acquisition, X.L.; data analysis, Y.Z., Y.L. (Yunqing Liu), N.L. and Z.G.; experiment, Y.L. (Yixin Li). All authors have read and agreed to the published version of the manuscript.

**Funding:** This research was funded by the Guangxi Key Research and Development Program funding, grant number AB19245045, open research fund of State Key Laboratory of Bioelectronics, Southeast University, grant number Sklb2021-k02, and open research fund program of Guangxi Key Lab of Mangrove Conservation and Utilization, grant number GKLMC-202002.

**Institutional Review Board Statement:** Not applicable.

**Informed Consent Statement:** Not applicable.

**Data Availability Statement:** The data (reef-building coral holobionts full-length and short-read transcriptome sequencing raw data) presented in this study are openly available in SRA at <https://www.ncbi.nlm.nih.gov/sra> (accessed on 18 September 2022). The reference numbers are SRR9613489 and SRR12904788-90 for *Pocillopora damicornis*; SRR12963486, SRR12959228, and SRR12959239-40 for *Pocillopora verrucosa*; SRR12963485, SRR12959195, SRR12959206, and SRR12959217 for *Acropora muricata*; and SRR12963484 and SRR12959182-4 for *Montipora foliosa*. The data (Unigene, CDS, PEP, and UTR sequences) analyzed in this study are openly available in Figshare at <https://doi.org/10.6084/m9.figshare.19403021> (accessed on 18 September 2022).

**Acknowledgments:** We thank M. Zhu from the Nanjing Institute of Geology and Paleontology, CAS for scientific guidance; M. Zhu, J. Lu, and Z. Gai from the Institute of Vertebrate Paleontology and Paleoanthropology; CAS for technical and scientific guidance; and Y. Loya from the Israel Academy of Sciences for scientific guidance.

**Conflicts of Interest:** The authors declare no conflict of interest.

## References

1. Hoegh-Guldberg, O. Climate change, coral bleaching and the future of the world's coral reefs. *Mar. Freshw. Res.* **1999**, *50*, 839. [[CrossRef](#)]

2. Copper, P. Ancient reef ecosystem expansion and collapse. *Coral Reefs* **1994**, *13*, 3–11. [[CrossRef](#)]
3. Reaka-Kudla, M.L. The global biodiversity of coral reefs: A comparison with rain forests. In *Biodiversity II: Understanding and Protecting our Biological Resources*; Reaka-Kudla, M.L., Wilson, D.E., Wilson, E.O., Eds.; Joseph Henry/National Academy Press: Washington, DC, USA, 1997; pp. 83–108.
4. Smith, S.V. Coral-reef area and the contributions of reefs to processes and resources of the world's oceans. *Nature* **1978**, *273*, 225–226. [[CrossRef](#)]
5. Spalding, M.D.; Grenfell, A.M. New estimates of global and regional coral reef areas. *Coral Reefs* **1997**, *16*, 225–230. [[CrossRef](#)]
6. Carpenter, K.E.; Abrar, M.; Aeby, G.; Aronson, R.B.; Banks, S.; Bruckner, A.; Chiriboga, A.; Cortes, J.; Delbeek, J.C.; Devantier, L.; et al. One-Third of Reef-Building Corals Face Elevated Extinction Risk from Climate Change and Local Impacts. *Science* **2008**, *321*, 560–563. [[CrossRef](#)]
7. Moberg, F.; Folke, C. Ecological goods and services of coral reef ecosystems. *Ecol. Econ.* **1999**, *29*, 215–233. [[CrossRef](#)]
8. Normile, D. Bringing Coral Reefs Back From the Living Dead. *Science* **2009**, *325*, 559–561. [[CrossRef](#)]
9. Wilkinson, C. *Status of Coral Reefs of the World: 2008 Global Coral Reef Monitoring Network and Reef and Rainforest Research Centre*; Global Coral Reef Monitoring Network and Reef and Rainforest Research Centre: Townsville, QLD, Australia, 2008; Volume 296.
10. Yu, K. Coral reefs in the South China Sea: Their response to and records on past environmental changes. *Sci. China Earth Sci.* **2012**, *55*, 1217–1229. [[CrossRef](#)]
11. Miller, D.J.; Ball, E.E.; Technau, U. Cnidarians and ancestral genetic complexity in the animal kingdom. *Trends Genet.* **2005**, *21*, 536–539. [[CrossRef](#)]
12. Finnerty, J.R. Origins of Bilateral Symmetry: Hox and Dpp Expression in a Sea Anemone. *Science* **2004**, *304*, 1335–1337. [[CrossRef](#)]
13. Genikhovich, G.; Technau, U. On the evolution of bilaterality. *Development* **2017**, *144*, 3392–3404. [[CrossRef](#)] [[PubMed](#)]
14. Falini, G.; Fermani, S.; Goffredo, S. Coral biomineralization: A focus on intra-skeletal organic matrix and calcification. *Semin. Cell Dev. Biol.* **2015**, *46*, 17–26. [[CrossRef](#)]
15. Allemand, D.; Tambutté, É.; Zoccola, D.; Tambutté, S. Coral Calcification, Cells to Reefs. In *Coral Reefs: An Ecosystem in Transition*; Springer: Berlin/Heidelberg, Germany, 2011; pp. 119–150.
16. Aranda, M.; Li, Y.; Liew, Y.J.; Baumgarten, S.; Simakov, O.; Wilson, M.C.; Piel, J.; Ashoor, H.; Bougouffa, S.; Bajic, V.B.; et al. Genomes of coral dinoflagellate symbionts highlight evolutionary adaptations conducive to a symbiotic lifestyle. *Sci. Rep.* **2016**, *6*, 39734. [[CrossRef](#)]
17. Gonzalez-Pech, R.A.; Stephens, T.G.; Chen, Y.B.; Mohamed, A.R.; Cheng, Y.Y.; Shah, S.; Dougan, K.E.; Fortuin, M.D.A.; Lagorce, R.; Burt, D.W.; et al. Comparison of 15 dinoflagellate genomes reveals extensive sequence and structural divergence in family Symbiodiniaceae and genus Symbiodinium. *BMC Biol.* **2021**, *19*, 73. [[CrossRef](#)] [[PubMed](#)]
18. Lin, S.; Cheng, S.; Song, B.; Zhong, X.; Lin, X.; Li, W.; Li, L.; Zhang, Y.; Zhang, H.; Ji, Z.; et al. The *Symbiodinium kawagutii* genome illuminates dinoflagellate gene expression and coral symbiosis. *Science* **2015**, *350*, 691–694. [[CrossRef](#)] [[PubMed](#)]
19. Liu, H.L.; Stephens, T.G.; Gonzalez-Pech, R.A.; Beltran, V.H.; Lapeyre, B.; Bongaerts, P.; Cooke, I.; Aranda, M.; Bourne, D.G.; Foret, S.; et al. Symbiodinium genomes reveal adaptive evolution of functions related to coral-dinoflagellate symbiosis. *Commun. Biol.* **2018**, *1*, 95. [[CrossRef](#)]
20. Shoguchi, E.; Beedessee, G.; Tada, I.; Hisata, K.; Kawashima, T.; Takeuchi, T.; Arakaki, N.; Fujie, M.; Koyanagi, R.; Roy, M.C.; et al. Two divergent Symbiodinium genomes reveal conservation of a gene cluster for sunscreen biosynthesis and recently lost genes. *BMC Genom.* **2018**, *19*, 458. [[CrossRef](#)]
21. Shoguchi, E.; Shinzato, C.; Kawashima, T.; Gyoja, F.; Mungpakdee, S.; Koyanagi, R.; Takeuchi, T.; Hisata, K.; Tanaka, M.; Fujiwara, M.; et al. Draft assembly of the *Symbiodinium minutum* nuclear genome reveals dinoflagellate gene structure. *Curr. Biol.* **2013**, *23*, 1399–1408. [[CrossRef](#)]
22. Gardner, S.G.; Camp, E.F.; Smith, D.J.; Kahlke, T.; Osman, E.O.; Gendron, G.; Hume, B.C.C.; Pogoreutz, C.; Voolstra, C.R.; Suggett, D.J. Coral microbiome diversity reflects mass coral bleaching susceptibility during the 2016 El Nino heat wave. *Ecol. Evol.* **2019**, *9*, 938–956. [[CrossRef](#)]
23. Zhou, Z.; Zhang, G.; Chen, G.; Ni, X.; Guo, L.; Yu, X.; Xiao, C.; Xu, Y.; Shi, X.; Huang, B. Elevated ammonium reduces the negative effect of heat stress on the stony coral *Pocillopora damicornis*. *Mar. Pollut. Bull.* **2017**, *118*, 319–327. [[CrossRef](#)]
24. Zhang, Y.; Zhou, Z.; Wang, L.; Huang, B. Transcriptome, expression, and activity analyses reveal a vital heat shock protein 70 in the stress response of stony coral *Pocillopora damicornis*. *Cell Stress Chaperones* **2018**, *23*, 711–721. [[CrossRef](#)] [[PubMed](#)]
25. Mollica, N.R.; Guo, W.; Cohen, A.L.; Huang, K.F.; Foster, G.L.; Donald, H.K.; Solow, A.R. Ocean acidification affects coral growth by reducing skeletal density. *Proc. Natl. Acad. Sci. USA* **2018**, *115*, 1754–1759. [[CrossRef](#)] [[PubMed](#)]
26. Kline, D.I.; Teneva, L.; Okamoto, D.K.; Schneider, K.; Caldeira, K.; Miard, T.; Chai, A.; Marker, M.; Dunbar, R.B.; Mitchell, B.G.; et al. Living coral tissue slows skeletal dissolution related to ocean acidification. *Nat. Ecol. Evol.* **2019**, *3*, 1438–1444. [[CrossRef](#)]
27. Hu, M.; Zheng, X.; Fan, C.M.; Zheng, Y. Lineage dynamics of the endosymbiotic cell type in the soft coral *Xenia*. *Nature* **2020**, *582*, 534–538. [[CrossRef](#)] [[PubMed](#)]
28. Levy, S.; Elek, A.; Grau-Bové, X.; Menéndez-Bravo, S.; Iglesias, M.; Tanay, A.; Mass, T.; Sebe-Pedros, A. A stony coral cell atlas illuminates the molecular and cellular basis of coral symbiosis, calcification, and immunity. *Cell* **2021**, *184*, 2973–2987. [[CrossRef](#)] [[PubMed](#)]
29. Orgel, J.; Sella, I.; Madhurapantula, R.S.; Antipova, O.; Mandelberg, Y.; Kashman, Y.; Benayahu, D.; Benayahu, Y. Molecular and ultrastructural studies of a fibrillar collagen from octocoral (Cnidaria). *J. Exp. Biol.* **2017**, *220*, 3327–3335. [[CrossRef](#)]

30. Tang, J.; Ni, X.; Zhou, Z.; Wang, L.; Lin, S. Acute microplastic exposure raises stress response and suppresses detoxification and immune capacities in the scleractinian coral *Pocillopora damicornis*. *Environ. Pollut.* **2018**, *243*, 66–74. [[CrossRef](#)]
31. Zhou, Z.; Zhao, S.; Tang, J.; Liu, Z.; Wu, Y.; Wang, Y.; Lin, S. Altered Immune Landscape and Disrupted Coral-Symbiodinium Symbiosis in the Scleractinian Coral *Pocillopora damicornis* by *Vibrio corallilyticus* Challenge. *Front. Physiol.* **2019**, *10*, 366. [[CrossRef](#)]
32. Cunning, R.; Bay, R.A.; Gillette, P.; Baker, A.C.; Traylor-Knowles, N. Comparative analysis of the *Pocillopora damicornis* genome highlights role of immune system in coral evolution. *Sci. Rep.* **2018**, *8*, 16134. [[CrossRef](#)]
33. Guo, Z.J.; Liao, X.; Chen, J.Y.; He, C.P.; Lu, Z.H. Binding Pattern Reconstructions of FGF-FGFR Budding-Inducing Signaling in Reef-Building Corals. *Front. Physiol.* **2022**, *12*, 759370. [[CrossRef](#)]
34. Li, Y.X.; Han, T.Y.; Bi, K.; Liang, K.; Chen, J.Y.; Lu, J.; He, C.P.; Lu, Z.H. The 3D Reconstruction of *Pocillopora* Colony Sheds Light on the Growth Pattern of This Reef-Building Coral. *iScience* **2020**, *23*, 101069. [[CrossRef](#)] [[PubMed](#)]
35. Shoguchi, E.; Tanaka, M.; Shinzato, C.; Kawashima, T.; Satoh, N. A genome-wide survey of photoreceptor and circadian genes in the coral, *Acropora digitifera*. *Gene* **2013**, *515*, 426–431. [[CrossRef](#)] [[PubMed](#)]
36. Levy, O.; Appelbaum, L.; Leggat, W.; Gothliff, Y.; Hayward, D.C.; Miller, D.J.; Hoegh-Guldberg, O. Light-responsive cryptochromes from a simple multicellular animal, the coral *Acropora millepora*. *Science* **2007**, *318*, 467–470. [[CrossRef](#)]
37. Vize, P.D. Transcriptome analysis of the circadian regulatory network in the coral *Acropora millepora*. *Biol. Bull.* **2009**, *216*, 131–137. [[CrossRef](#)] [[PubMed](#)]
38. Wang, X.; Zoccola, D.; Liew, Y.J.; Tambutte, E.; Cui, G.; Allemand, D.; Tambutte, S.; Aranda, M. The Evolution of Calcification in Reef-Building Corals. *Mol. Biol. Evol.* **2021**, *38*, 3543–3555. [[CrossRef](#)] [[PubMed](#)]
39. Zoccola, D.; Tambutte, E.; Kulhanek, E.; Puverel, S.; Scimeca, J.C.; Allemand, D.; Tambutte, S. Molecular cloning and localization of a PMCA P-type calcium ATPase from the coral *Stylophora pistillata*. *Biochim. Biophys. Acta* **2004**, *1663*, 117–126. [[CrossRef](#)]
40. Zoccola, D.; Tambutte, E.; Senegas-Balas, F.; Michiels, J.F.; Failla, J.P.; Jaubert, J.; Allemand, D. Cloning of a calcium channel alpha1 subunit from the reef-building coral, *Stylophora pistillata*. *Gene* **1999**, *227*, 157–167. [[CrossRef](#)]
41. Bertucci, A.; Moya, A.; Tambutte, S.; Allemand, D.; Supuran, C.T.; Zoccola, D. Carbonic anhydrases in anthozoan corals—A review. *Bioorg. Med. Chem.* **2013**, *21*, 1437–1450. [[CrossRef](#)]
42. Venn, A.A.; Tambutte, E.; Lotto, S.; Zoccola, D.; Allemand, D.; Tambutte, S. Imaging intracellular pH in a reef coral and symbiotic anemone. *Proc. Natl. Acad. Sci. USA* **2009**, *106*, 16574–16579. [[CrossRef](#)]
43. Hopkinson, B.M.; Tansik, A.L.; Fitt, W.K. Internal carbonic anhydrase activity in the tissue of scleractinian corals is sufficient to support proposed roles in photosynthesis and calcification. *J. Exp. Biol.* **2015**, *218*, 2039–2048. [[CrossRef](#)]
44. Zoccola, D.; Ganot, P.; Bertucci, A.; Caminiti-Segonds, N.; Techer, N.; Voolstra, C.R.; Aranda, M.; Tambutte, E.; Allemand, D.; Casey, J.R.; et al. Bicarbonate transporters in corals point towards a key step in the evolution of cnidarian calcification. *Sci. Rep.* **2015**, *5*, 9983. [[CrossRef](#)] [[PubMed](#)]
45. Mass, T.; Drake, L.J.; Haramaty, L.J.; Zelzion, E.; Bhattacharya, D.; Falkowski, P.G. Cloning and Characterization of Four Novel Coral Acid-Rich Proteins that Precipitate Carbonates In Vitro. *Curr. Biol.* **2013**, *23*, 1126–1131. [[CrossRef](#)] [[PubMed](#)]
46. Puverel, S.; Tambutte, E.; Pereira-Mouries, L.; Zoccola, D.; Allemand, D.; Tambutte, S. Soluble organic matrix of two Scleractinian corals: Partial and comparative analysis. *Comp. Biochem. Physiol. B Biochem. Mol. Biol.* **2005**, *141*, 480–487. [[CrossRef](#)]
47. Bhattacharya, D.; Agrawal, S.; Aranda, M.; Baumgarten, S.; Belcaid, M.; Drake, J.L.; Erwin, D.; Foret, S.; Gates, R.D.; Gruber, D.F.; et al. Comparative genomics explains the evolutionary success of reef-forming corals. *eLife* **2016**, *5*, e13288. [[CrossRef](#)]
48. Drake, J.L.; Mass, T.; Haramaty, L.; Zelzion, E.; Bhattacharya, D.; Falkowski, P.G. Proteomic analysis of skeletal organic matrix from the stony coral *Stylophora pistillata*. *Proc. Natl. Acad. Sci. USA* **2013**, *110*, 3788–3793. [[CrossRef](#)]
49. Ramos-Silva, P.; Kaandorp, J.; Huisman, L.; Marie, B.; Zanella-Cleon, I.; Guichard, N.; Miller, D.J.; Marin, F. The skeletal proteome of the coral *Acropora millepora*: The evolution of calcification by co-option and domain shuffling. *Mol. Biol. Evol.* **2013**, *30*, 2099–2112. [[CrossRef](#)]
50. Brocks, J.J.; Jarrett, A.J.M.; Sirantoine, E.; Hallmann, C.; Hoshino, Y.; Liyanage, T. The rise of algae in Cryogenian oceans and the emergence of animals. *Nature* **2017**, *548*, 578–581. [[CrossRef](#)]
51. Mills, D.B. The origin of phagocytosis in Earth history. *Interface Focus* **2020**, *10*, 20200019. [[CrossRef](#)]
52. Knoll, A.H. Biogeochemistry: Food for early animal evolution. *Nature* **2017**, *548*, 528–530. [[CrossRef](#)]
53. Cong, P.; Ma, X.; Williams, M.; Siveter, D.J.; Siveter, D.J.; Gabbott, S.E.; Zhai, D.; Goral, T.; Edgecombe, G.D.; Hou, X. Host-specific infestation in early Cambrian worms. *Nat. Ecol. Evol.* **2017**, *1*, 1465–1469. [[CrossRef](#)]
54. Davy, S.K.; Allemand, D.; Weis, V.M. Cell Biology of Cnidarian-Dinoflagellate Symbiosis. *Microbiol. Mol. Biol. Rev.* **2012**, *76*, 229–261. [[CrossRef](#)] [[PubMed](#)]
55. Sebe-Pedros, A.; Saudemont, B.; Chomsky, E.; Plessier, F.; Mailhe, M.P.; Renno, J.; Loe-Mie, Y.; Lifshitz, A.; Mukamel, Z.; Schmutz, S.; et al. Cnidarian Cell Type Diversity and Regulation Revealed by Whole-Organism Single-Cell RNA-Seq. *Cell* **2018**, *173*, 1520–1534. [[CrossRef](#)]
56. Guibert, I.; Lecellier, G.; Torda, G.; Pochon, X.; Berteaux-Lecellier, V. Metabarcoding reveals distinct microbiotypes in the giant clam *Tridacna maxima*. *Microbiome* **2020**, *8*, 57. [[CrossRef](#)] [[PubMed](#)]
57. Weis, V.M. Cell Biology of Coral Symbiosis: Foundational Study Can Inform Solutions to the Coral Reef Crisis. *Integr. Comp. Biol.* **2019**, *59*, 845–855. [[CrossRef](#)] [[PubMed](#)]
58. Kobayashi, J.; Kubota, T. Bioactive macrolides and polyketides from marine dinoflagellates of the genus *Amphidinium*. *J. Nat. Prod.* **2007**, *70*, 451–460. [[CrossRef](#)]

59. Murata, M.; Yasumoto, T. The structure elucidation and biological activities of high molecular weight algal toxins: Maitotoxin, prymnesins and zooxanthellatoxins. *Nat. Prod. Rep.* **2000**, *17*, 293–314. [CrossRef]
60. Hellyer, S.D. Chapter Four—Marine-derived nicotinic receptor antagonist toxins: Pinnatoxins and alpha conotoxins. In *Advances in Neurotoxicology*; Novelli, A., Fernández-Sánchez, M.-T., Aschner, M., Costa, L.G., Eds.; Academic Press: Cambridge, MA, USA, 2021; Volume 6, pp. 105–191.
61. Dunn, C.W.; Hejnol, A.; Matus, D.Q.; Pang, K.; Browne, W.E.; Smith, S.A.; Seaver, E.; Rouse, G.W.; Obst, M.; Edgecombe, G.D.; et al. Broad phylogenomic sampling improves resolution of the animal tree of life. *Nature* **2008**, *452*, 745–749. [CrossRef]
62. Ryan, J.F.; Pang, K.; Schnitzler, C.E.; Nguyen, A.D.; Moreland, R.T.; Simmons, D.K.; Koch, B.J.; Francis, W.R.; Havlak, P.; Program, N.C.S.; et al. The genome of the ctenophore *Mnemiopsis leidyi* and its implications for cell type evolution. *Science* **2013**, *342*, 1242592. [CrossRef]
63. Moroz, L.L.; Kocot, K.M.; Citarella, M.R.; Dosung, S.; Norekian, T.P.; Povolotskaya, I.S.; Grigorenko, A.P.; Dailey, C.; Berezikov, E.; Buckley, K.M.; et al. The ctenophore genome and the evolutionary origins of neural systems. *Nature* **2014**, *510*, 109–114. [CrossRef]
64. Whelan, N.V.; Kocot, K.M.; Moroz, L.L.; Halanych, K.M. Error, signal, and the placement of Ctenophora sister to all other animals. *Proc. Natl. Acad. Sci. USA* **2015**, *112*, 5773–5778. [CrossRef]
65. Pisani, D.; Pett, W.; Dohrmann, M.; Feuda, R.; Rota-Stabelli, O.; Philippe, H.; Lartillot, N.; Worheide, G. Genomic data do not support comb jellies as the sister group to all other animals. *Proc. Natl. Acad. Sci. USA* **2015**, *112*, 15402–15407. [CrossRef] [PubMed]
66. Simion, P.; Philippe, H.; Baurain, D.; Jager, M.; Richter, D.J.; Di Franco, A.; Roure, B.; Satoh, N.; Queinsec, E.; Ereskovsky, A.; et al. A Large and Consistent Phylogenomic Dataset Supports Sponges as the Sister Group to All Other Animals. *Curr. Biol.* **2017**, *27*, 958–967. [CrossRef] [PubMed]
67. Feuda, R.; Dohrmann, M.; Pett, W.; Philippe, H.; Rota-Stabelli, O.; Lartillot, N.; Worheide, G.; Pisani, D. Improved Modeling of Compositional Heterogeneity Supports Sponges as Sister to All Other Animals. *Curr. Biol.* **2017**, *27*, 3864–3870.e3864. [CrossRef] [PubMed]
68. Redmond, A.K.; McLysaght, A. Evidence for sponges as sister to all other animals from partitioned phylogenomics with mixture models and recoding. *Nat. Commun.* **2021**, *12*, 1783. [CrossRef]
69. Reitzel, A.M.; Behrendt, L.; Tarrant, A.M. Light Entrained Rhythmic Gene Expression in the Sea Anemone *Nematostella vectensis*: The Evolution of the Animal Circadian Clock. *PLoS ONE* **2010**, *5*, e12805. [CrossRef]
70. Jindrich, K.; Roper, K.E.; Lemon, S.; Degnan, B.M.; Reitzel, A.M.; Degnan, S.M. Origin of the Animal Circadian Clock: Diurnal and Light-Entrained Gene Expression in the Sponge *Amphimedon queenslandica*. *Front. Mar. Sci.* **2017**, *4*, 327. [CrossRef]
71. Sasson, D.A.; Ryan, J.F. The sex lives of ctenophores: The influence of light, body size, and self-fertilization on the reproductive output of the sea walnut, *Mnemiopsis leidyi*. *PeerJ* **2016**, *4*, e1846. [CrossRef]
72. Lowrey, P.L.; Takahashi, J.S. Mammalian circadian biology: Elucidating genome-wide levels of temporal organization. *Annu. Rev. Genom. Hum. Genet.* **2004**, *5*, 407–441. [CrossRef]
73. Yang, Z.; Liu, B.; Su, J.; Liao, J.; Lin, C.; Oka, Y. Cryptochromes Orchestrate Transcription Regulation of Diverse Blue Light Responses in Plants. *Photochem. Photobiol.* **2017**, *93*, 112–127. [CrossRef]
74. Dunlap, J.C. Molecular bases for circadian clocks. *Cell* **1999**, *96*, 271–290. [CrossRef]
75. Krishnan, B.; Levine, J.D.; Lynch, M.K.S.; Dowse, H.B.; Funes, P.; Hall, J.C.; Hardin, P.E.; Dryer, S.E. A new role for cryptochrome in a *Drosophila* circadian oscillator. *Nature* **2001**, *411*, 313–317. [CrossRef] [PubMed]
76. Griffin, E.A., Jr.; Staknis, D.; Weitz, C.J. Light-independent role of CRY1 and CRY2 in the mammalian circadian clock. *Science* **1999**, *286*, 768–771. [CrossRef] [PubMed]
77. Zhu, H.S.; Sauman, I.; Yuan, Q.; Casselman, A.; Emery-Le, M.; Emery, P.; Reppert, S.M. Cryptochromes define a novel circadian clock mechanism in monarch butterflies that may underlie sun compass navigation. *PLoS Biol.* **2008**, *6*, 138–155. [CrossRef]
78. Zhu, H.; Yuan, Q.; Briscoe, A.D.; Froy, O.; Casselman, A.; Reppert, S.M. The two CRYs of the butterfly. *Curr. Biol.* **2005**, *15*, R953–R954. [CrossRef] [PubMed]
79. Hoeksema, B.W.; Rogers, A.; Quibilan, M.C. *Pocillopora damicornis*. The IUCN Red List of Threatened Species 2014: E.T133222A54216898. Available online: <https://doi.org/10.2305/IUCN.UK.2014-1.RLTS.T133222A54216898.en> (accessed on 1 August 2022).
80. Richards, Z.T.; Delbeek, J.T.; Lovell, E.R.; Bass, D.; Aeby, G.; Reboton, C. *Acropora formosa*. The IUCN Red List of Threatened Species 2014: E.T133644A54299282. Available online: <https://doi.org/10.2305/IUCN.UK.2014-1.RLTS.T133644A54299282.en> (accessed on 1 August 2022).
81. DeVantier, L.; Hodgson, G.; Huang, D.; Johan, O.; Licuanan, A.; Obura, D.O. *Montipora foliosa*. The IUCN Red List of Threatened Species 2014: E.T133071A54189890. Available online: <https://doi.org/10.2305/IUCN.UK.2014-1.RLTS.T133071A54189890.en> (accessed on 1 August 2022).
82. Hoeksema, B.W.; Rogers, A.; Quibilan, M.C. *Pocillopora verrucosa*. The IUCN Red List of Threatened Species 2014: E.T133197A54210095. Available online: <https://doi.org/10.2305/IUCN.UK.2014-1.RLTS.T133197A54210095.en> (accessed on 1 August 2022).
83. Van Dijk, E.L.; Jaszczyszyn, Y.; Naquin, D.; Thermes, C. The Third Revolution in Sequencing Technology. *Trends Genet.* **2018**, *34*, 666–681. [CrossRef]

84. Lu, H.; Giordano, F.; Ning, Z. Oxford Nanopore MinION Sequencing and Genome Assembly. *Genom. Proteom. Bioinform.* **2016**, *14*, 265–279. [[CrossRef](#)]
85. Rhoads, A.; Au, K.F. PacBio Sequencing and Its Applications. *Genom. Proteom. Bioinform.* **2015**, *13*, 278–289. [[CrossRef](#)]
86. Vidal-Dupiol, J.; Zoccola, D.; Tambutté, E.; Grunau, C.; Cosseau, C.; Smith, K.M.; Freitag, M.; Dheilily, N.M.; Allemand, D.; Tambutté, S. Genes Related to Ion-Transport and Energy Production Are Upregulated in Response to CO<sub>2</sub>-Driven pH Decrease in Corals: New Insights from Transcriptome Analysis. *PLoS ONE* **2013**, *8*, e58652. [[CrossRef](#)]
87. Mayfield, A.B.; Wang, Y.B.; Chen, C.S.; Lin, C.Y.; Chen, S.H. Compartment-specific transcriptomics in a reef-building coral exposed to elevated temperatures. *Mol. Ecol.* **2014**, *23*, 5816–5830. [[CrossRef](#)] [[PubMed](#)]
88. Yuan, C.; Zhou, Z.; Zhang, Y.; Chen, G.; Yu, X.; Ni, X.; Tang, J.; Huang, B. Effects of elevated ammonium on the transcriptome of the stony coral *Pocillopora damicornis*. *Mar. Pollut. Bull.* **2017**, *114*, 46–52. [[CrossRef](#)]
89. Zhou, Z.; Yu, X.; Tang, J.; Wu, Y.; Wang, L.; Huang, B. Systemic response of the stony coral *Pocillopora damicornis* against acute cadmium stress. *Aquat. Toxicol.* **2018**, *194*, 132–139. [[CrossRef](#)] [[PubMed](#)]
90. Mass, T.; Putnam, H.M.; Drake, J.L.; Zelzion, E.; Gates, R.D.; Bhattacharya, D.; Falkowski, P.G. Temporal and spatial expression patterns of biomineralization proteins during early development in the stony coral *Pocillopora damicornis*. *Proc. Biol. Sci.* **2016**, *283*, 20160322. [[CrossRef](#)] [[PubMed](#)]
91. Crowder, C.M.; Meyer, E.; Fan, T.Y.; Weis, V.M. Impacts of temperature and lunar day on gene expression profiles during a monthly reproductive cycle in the brooding coral *Pocillopora damicornis*. *Mol. Ecol.* **2017**, *26*, 3913–3925. [[CrossRef](#)] [[PubMed](#)]
92. Wecker, P.; Lecellier, G.; Guibert, I.; Zhou, Y.; Bonnard, I.; Berteaux-Lecellier, V. Exposure to the environmentally-persistent insecticide chlordecone induces detoxification genes and causes polyp bail-out in the coral *P. damicornis*. *Chemosphere* **2018**, *195*, 190–200. [[CrossRef](#)]
93. Johnston, E.C.; Forsman, Z.H.; Flot, J.-F.; Schmidt-Roach, S.; Pinzón, J.H.; Knapp, I.S.S.; Toonen, R.J. A genomic glance through the fog of plasticity and diversification in *Pocillopora*. *Sci. Rep.* **2017**, *7*, 5991. [[CrossRef](#)]
94. Quattrini, A.M.; Faircloth, B.C.; Duenas, L.F.; Bridge, T.C.L.; Brugler, M.R.; Calixto-Botia, I.F.; DeLeo, D.M.; Foret, S.; Herrera, S.; Lee, S.M.Y.; et al. Universal target-enrichment baits for anthozoan (Cnidaria) phylogenomics: New approaches to long-standing problems. *Mol. Ecol. Resour.* **2018**, *18*, 281–295. [[CrossRef](#)]
95. Flot, J.F.; Tillier, S. The mitochondrial genome of *Pocillopora* (Cnidaria: Scleractinia) contains two variable regions: The putative D-loop and a novel ORF of unknown function. *Gene* **2007**, *401*, 80–87. [[CrossRef](#)]
96. Walters, B.M.; Connelly, M.T.; Young, B.; Traylor-Knowles, N. The Complicated Evolutionary Diversification of the Mpeg-1/Perforin-2 Family in Cnidarians. *Front. Immunol.* **2020**, *11*, 1690. [[CrossRef](#)]
97. Morikawa, M.K.; Palumbi, S.R. Using naturally occurring climate resilient corals to construct bleaching-resistant nurseries. *Proc. Natl. Acad. Sci. USA* **2019**, *116*, 10586–10591. [[CrossRef](#)]
98. Buitrago-Lopez, C.; Mariappan, K.G.; Cardenas, A.; Gegner, H.M.; Voolstra, C.R. The Genome of the Cauliflower Coral *Pocillopora verrucosa*. *Genome Biol. Evol.* **2020**, *12*, 1911–1917. [[CrossRef](#)]
99. Lee, S.T.M.; Keshavmurthy, S.; Fontana, S.; Takuma, M.; Chou, W.H.; Chen, C.A. Transcriptomic response in *Acropora muricata* under acute temperature stress follows preconditioned seasonal temperature fluctuations. *BMC Res. Notes* **2018**, *11*, 119. [[CrossRef](#)] [[PubMed](#)]
100. Shinzato, C.; Khalturin, K.; Inoue, J.; Zayasu, Y.; Kanda, M.; Kawamitsu, M.; Yoshioka, Y.; Yamashita, H.; Suzuki, G.; Satoh, N. Eighteen Coral Genomes Reveal the Evolutionary Origin of Acropora Strategies to Accommodate Environmental Changes. *Mol. Biol. Evol.* **2021**, *38*, 16–30. [[CrossRef](#)] [[PubMed](#)]
101. Shinzato, C.; Zayasu, Y.; Kanda, M.; Kawamitsu, M.; Satoh, N.; Yamashita, H.; Suzuki, G. Using Seawater to Document Coral-Zoothanella Diversity: A New Approach to Coral Reef Monitoring Using Environmental DNA. *Front. Mar. Sci.* **2018**, *5*, 28. [[CrossRef](#)]
102. Ceh, J.; Raina, J.-B.; Soo, R.M.; Van Keulen, M.; Bourne, D.G. Coral-Bacterial Communities before and after a Coral Mass Spawning Event on Ningaloo Reef. *PLoS ONE* **2012**, *7*, e36920. [[CrossRef](#)]
103. Mhuantong, W.; Nuryadi, H.; Trianto, A.; Sabdono, A.; Tangphatsornruang, S.; Eurwilaichitr, L.; Kanokratana, P.; Champreda, V. Comparative analysis of bacterial communities associated with healthy and diseased corals in the Indonesian sea. *PeerJ* **2019**, *7*, e8137. [[CrossRef](#)]
104. Diaz, J.M.; Hansel, C.M.; Apprill, A.; Brighi, C.; Zhang, T.; Weber, L.; McNally, S.; Xun, L. Species-specific control of external superoxide levels by the coral holobiont during a natural bleaching event. *Nat. Commun.* **2016**, *7*, 13801. [[CrossRef](#)]
105. Beatty, D.S.; Clements, C.S.; Stewart, F.J.; Hay, M.E. Intergenerational effects of macroalgae on a reef coral: Major declines in larval survival but subtle changes in microbiomes. *Mar. Ecol. Prog. Ser.* **2018**, *589*, 97–114. [[CrossRef](#)]
106. Beatty, D.S.; Valayil, J.M.; Clements, C.S.; Ritchie, K.B.; Stewart, F.J.; Hay, M.E. Variable effects of local management on coral defenses against a thermally regulated bleaching pathogen. *Sci. Adv.* **2019**, *5*, eaay1048. [[CrossRef](#)]
107. Epstein, H.E.; Torda, G.; Munday, P.L.; van Oppen, M.J.H. Parental and early life stage environments drive establishment of bacterial and dinoflagellate communities in a common coral. *ISME J.* **2019**, *13*, 1635–1638. [[CrossRef](#)]
108. Van Oppen, M.J.H.; Bongaerts, P.; Frade, P.; Peplow, L.M.; Boyd, S.E.; Nim, H.T.; Bay, L.K. Adaptation to reef habitats through selection on the coral animal and its associated microbiome. *Mol. Ecol.* **2018**, *27*, 2956–2971. [[CrossRef](#)]

109. Osman, E.O.; Suggett, D.J.; Voolstra, C.R.; Pettay, D.T.; Clark, D.R.; Pogoreutz, C.; Sampayo, E.M.; Warner, M.E.; Smith, D.J. Coral microbiome composition along the northern Red Sea suggests high plasticity of bacterial and specificity of endosymbiotic dinoflagellate communities. *Microbiome* **2020**, *8*, 8. [[CrossRef](#)] [[PubMed](#)]
110. Li, J.; Long, L.; Zou, Y.; Zhang, S. Microbial community and transcriptional responses to increased temperatures in coral *Pocillopora damicornis* holobiont. *Environ. Microbiol.* **2021**, *23*, 826–843. [[CrossRef](#)]
111. Brener-Raffalli, K.; Clerissi, C.; Vidal-Dupiol, J.; Adjeroud, M.; Bonhomme, F.; Pratlong, M.; Aurelle, D.; Mitta, G.; Toulza, E. Thermal regime and host clade, rather than geography, drive Symbiodinium and bacterial assemblages in the scleractinian coral *Pocillopora damicornis* sensu lato. *Microbiome* **2018**, *6*, 39. [[CrossRef](#)] [[PubMed](#)]
112. Chen, B.; Yu, K.; Liao, Z.; Yu, X.; Qin, Z.; Liang, J.; Wang, G.; Wu, Q.; Jiang, L. Microbiome community and complexity indicate environmental gradient acclimatisation and potential microbial interaction of endemic coral holobionts in the South China Sea. *Sci. Total Environ.* **2021**, *765*, 142690. [[CrossRef](#)] [[PubMed](#)]
113. Sun, F.; Yang, H.; Wang, G.; Shi, Q. Combination Analysis of Metatranscriptome and Metagenome Reveal the Composition and Functional Response of Coral Symbionts to Bleaching During an El Nino Event. *Front. Microbiol.* **2020**, *11*, 448. [[CrossRef](#)] [[PubMed](#)]
114. Ziegler, M.; Grupstra, C.G.B.; Barreto, M.M.; Eaton, M.; BaOmar, J.; Zubier, K.; Al-Sofyani, A.; Turki, A.J.; Ormond, R.; Voolstra, C.R. Coral bacterial community structure responds to environmental change in a host-specific manner. *Nat. Commun.* **2019**, *10*, 3092. [[CrossRef](#)] [[PubMed](#)]
115. Yang, Q.; Zhang, Y.; Ahmad, M.; Ling, J.; Zhou, W.; Zhang, Y.; Dong, J. Microbial community structure shifts and potential Symbiodinium partner bacterial groups of bleaching coral *Pocillopora verrucosa* in South China Sea. *Ecotoxicology* **2021**, *30*, 966–974. [[CrossRef](#)]
116. Pogoreutz, C.; Radecker, N.; Cardenas, A.; Gardes, A.; Wild, C.; Voolstra, C.R. Dominance of Endozoicomonas bacteria throughout coral bleaching and mortality suggests structural inflexibility of the *Pocillopora verrucosa* microbiome. *Ecol. Evol.* **2018**, *8*, 2240–2252. [[CrossRef](#)]
117. Neave, M.J.; Michell, C.T.; Apprill, A.; Voolstra, C.R. Endozoicomonas genomes reveal functional adaptation and plasticity in bacterial strains symbiotically associated with diverse marine hosts. *Sci. Rep.* **2017**, *7*, 40579. [[CrossRef](#)]
118. Ziegler, M.; Roik, A.; Porter, A.; Zubier, K.; Mudarris, M.S.; Ormond, R.; Voolstra, C.R. Coral microbial community dynamics in response to anthropogenic impacts near a major city in the central Red Sea. *Mar. Pollut. Bull.* **2016**, *105*, 629–640. [[CrossRef](#)]
119. Neave, M.J.; Rachmawati, R.; Xun, L.; Michell, C.T.; Bourne, D.G.; Apprill, A.; Voolstra, C.R. Differential specificity between closely related corals and abundant *Endozoicomonas endosymbionts* across global scales. *ISME J.* **2017**, *11*, 186–200. [[CrossRef](#)] [[PubMed](#)]
120. Van de Water, J.A.J.M.; Courtial, L.; Houllbrèque, F.; Jacquet, S.; Ferrier-Pagès, C. Ultra-Violet Radiation Has a Limited Impact on Seasonal Differences in the Acropora Muricata Holobiont. *Front. Mar. Sci.* **2018**, *5*, 275. [[CrossRef](#)]
121. Sweet, M.; Bythell, J. White syndrome in Acropora muricata: Nonspecific bacterial infection and ciliate histophagy. *Mol. Ecol.* **2015**, *24*, 1150–1159. [[CrossRef](#)] [[PubMed](#)]
122. Tombacz, D.; Sharon, D.; Olah, P.; Csabai, Z.; Snyder, M.; Boldogkoi, Z. Strain Kaplan of Pseudorabies Virus Genome Sequenced by PacBio Single-Molecule Real-Time Sequencing Technology. *Genome Announc* **2014**, *2*, 1009–1017. [[CrossRef](#)]
123. Chin, C.S.; Alexander, D.H.; Marks, P.; Klammer, A.A.; Drake, J.; Heiner, C.; Clum, A.; Copeland, A.; Huddleston, J.; Eichler, E.E.; et al. Nonhybrid, finished microbial genome assemblies from long-read SMRT sequencing data. *Nat. Methods* **2013**, *10*, 563–569. [[CrossRef](#)]
124. Chen, S.; Qiu, G.; Yang, M. SMRT sequencing of full-length transcriptome of seagrasses *Zostera japonica*. *Sci. Rep.* **2019**, *9*, 14537. [[CrossRef](#)]
125. Zhang, S.J.; Wang, C.Q.; Yan, S.Y.; Fu, A.S.; Luan, X.K.; Li, Y.M.; Shen, Q.S.; Zhong, X.M.; Chen, J.Y.; Wang, X.F.; et al. Isoform Evolution in Primates through Independent Combination of Alternative RNA Processing Events. *Mol. Biol. Evol.* **2017**, *34*, 2453–2468. [[CrossRef](#)]
126. Weirather, J.L.; Afshar, P.T.; Clark, T.A.; Tseng, E.; Powers, L.S.; Underwood, J.G.; Zabner, J.; Korfach, J.; Wong, W.H.; Au, K.F. Characterization of fusion genes and the significantly expressed fusion isoforms in breast cancer by hybrid sequencing. *Nucleic Acids Res.* **2015**, *43*, e116. [[CrossRef](#)]
127. Huang, K.K.; Huang, J.W.; Wu, J.K.L.; Lee, M.H.; Tay, S.T.; Kumar, V.; Ramnarayanan, K.; Padmanabhan, N.; Xu, C.; Tan, A.L.K.; et al. Long-read transcriptome sequencing reveals abundant promoter diversity in distinct molecular subtypes of gastric cancer. *Genome Biol.* **2021**, *22*, 44. [[CrossRef](#)]
128. Naftaly, A.S.; Pau, S.; White, M.A. Long-read RNA sequencing reveals widespread sex-specific alternative splicing in threespine stickleback fish. *Genome Res.* **2021**, *31*, 1486–1497. [[CrossRef](#)]
129. Li, W.; Jaroszewski, L.; Godzik, A. Tolerating some redundancy significantly speeds up clustering of large protein databases. *Bioinformatics* **2002**, *18*, 77–82. [[CrossRef](#)]
130. Finn, R.D.; Coggill, P.; Eberhardt, R.Y.; Eddy, S.R.; Mistry, J.; Mitchell, A.L.; Potter, S.C.; Punta, M.; Qureshi, M.; Sangrador-Vegas, A.; et al. The Pfam protein families database: Towards a more sustainable future. *Nucleic Acids Res.* **2016**, *44*, D279–D285. [[CrossRef](#)] [[PubMed](#)]



131. Tatusov, R.L.; Fedorova, N.D.; Jackson, J.D.; Jacobs, A.R.; Kiryutin, B.; Koonin, E.V.; Krylov, D.M.; Mazumder, R.; Mekhedov, S.L.; Nikolskaya, A.N.; et al. The COG database: An updated version includes eukaryotes. *BMC Bioinform.* **2003**, *4*, 41. [[CrossRef](#)] [[PubMed](#)]
132. Bairoch, A.; Apweiler, R. The SWISS-PROT protein sequence database and its supplement TrEMBL in 2000. *Nucleic Acids Res.* **2000**, *28*, 45–48. [[CrossRef](#)] [[PubMed](#)]
133. Kanehisa, M.; Goto, S.; Kawashima, S.; Okuno, Y.; Hattori, M. The KEGG resource for deciphering the genome. *Nucleic Acids Res.* **2004**, *32*, D277–D280. [[CrossRef](#)] [[PubMed](#)]
134. Ashburner, M.; Ball, C.A.; Blake, J.A.; Botstein, D.; Butler, H.; Cherry, J.M.; Davis, A.P.; Dolinski, K.; Dwight, S.S.; Eppig, J.T.; et al. Gene ontology: Tool for the unification of biology. The Gene Ontology Consortium. *Nat. Genet.* **2000**, *25*, 25–29. [[CrossRef](#)] [[PubMed](#)]
135. Shumaker, A.; Putnam, H.M.; Qiu, H.; Price, D.C.; Zelzion, E.; Harel, A.; Wagner, N.E.; Gates, R.D.; Yoon, H.S.; Bhattacharya, D. Genome analysis of the rice coral *Montipora capitata*. *Sci. Rep.* **2019**, *9*, 2571. [[CrossRef](#)]
136. Shinzato, C.; Shoguchi, E.; Kawashima, T.; Hamada, M.; Hisata, K.; Tanaka, M.; Fujie, M.; Fujiwara, M.; Koyanagi, R.; Ikuta, T.; et al. Using the *Acropora digitifera* genome to understand coral responses to environmental change. *Nature* **2011**, *476*, 320–U382. [[CrossRef](#)]
137. Ying, H.; Hayward, D.C.; Cooke, I.; Wang, W.; Moya, A.; Siemering, K.R.; Sprungala, S.; Ball, E.E.; Foret, S.; Miller, D.J. The Whole-Genome Sequence of the Coral *Acropora millepora*. *Genome Biol. Evol.* **2019**, *11*, 1374–1379. [[CrossRef](#)]
138. Brawand, D.; Soumillon, M.; Necsulea, A.; Julien, P.; Csardi, G.; Harrigan, P.; Weier, M.; Liechti, A.; Aximu-Petri, A.; Kircher, M.; et al. The evolution of gene expression levels in mammalian organs. *Nature* **2011**, *478*, 343–348. [[CrossRef](#)]
139. Zhou, Y.; Zhu, J.; Tong, T.; Wang, J.; Lin, B.; Zhang, J. A statistical normalization method and differential expression analysis for RNA-seq data between different species. *BMC Bioinform.* **2019**, *20*, 163. [[CrossRef](#)]
140. Ying, H.; Cooke, I.; Sprungala, S.; Wang, W.; Hayward, D.C.; Tang, Y.; Huttley, G.; Ball, E.E.; Foret, S.; Miller, D.J. Comparative genomics reveals the distinct evolutionary trajectories of the robust and complex coral lineages. *Genome Biol.* **2018**, *19*, 175. [[CrossRef](#)] [[PubMed](#)]
141. Meibom, A.; Cuif, J.P.; Hillion, F.O.; Constantz, B.R.; Juillet-Leclerc, A.; Dauphin, Y.; Watanabe, T.; Dunbar, R.B. Distribution of magnesium in coral skeleton. *Geophys. Res. Lett.* **2004**, *31*, L23306. [[CrossRef](#)]
142. Li, Y.X.; Liao, X.; Bi, K.; Han, T.Y.; Chen, J.Y.; Lu, J.; He, C.P.; Lu, Z.H. Micro-CT reconstruction reveals the colony pattern regulations of four dominant reef-building corals. *Ecol. Evol.* **2021**, *11*, 16266–16279. [[CrossRef](#)] [[PubMed](#)]
143. Marat, A.L.; McPherson, P.S. The connecdenn family, Rab35 guanine nucleotide exchange factors interfacing with the clathrin machinery. *J. Biol. Chem.* **2010**, *285*, 10627–10637. [[CrossRef](#)]
144. Heisler, F.F.; Loeblich, S.; Pechmann, Y.; Maier, N.; Zivkovic, A.R.; Tokito, M.; Hausrat, T.J.; Schweizer, M.; Bähring, R.; Holzbaur, E.L.F.; et al. Musckelin Regulates Actin Filament- and Microtubule-Based GABA(A) Receptor Transport in Neurons. *Neuron* **2011**, *70*, 66–81. [[CrossRef](#)]
145. Kielty, C.M.; Baldock, C.; Lee, D.; Rock, M.J.; Ashworth, J.L.; Shuttleworth, C.A. Fibrillin: From microfibril assembly to biomechanical function. *Philos. Trans. R. Soc. B Biol. Sci.* **2002**, *357*, 207–217. [[CrossRef](#)]
146. Sommer, B.; Oprins, A.; Rabouille, C.; Munro, S. The exocyst component Sec5 is present on endocytic vesicles in the oocyte of *Drosophila melanogaster*. *J. Cell Biol.* **2005**, *169*, 953–963. [[CrossRef](#)]
147. Wu, T.D.; Watanabe, C.K. GMAP: A genomic mapping and alignment program for mRNA and EST sequences. *Bioinformatics* **2005**, *21*, 1859–1875. [[CrossRef](#)]
148. Salmela, L.; Rivals, E. LoRDEC: Accurate and efficient long read error correction. *Bioinformatics* **2014**, *30*, 3506–3514. [[CrossRef](#)]
149. Fu, L.; Niu, B.; Zhu, Z.; Wu, S.; Li, W. CD-HIT: Accelerated for clustering the next-generation sequencing data. *Bioinformatics* **2012**, *28*, 3150–3152. [[CrossRef](#)] [[PubMed](#)]
150. Altschul, S.F.; Gish, W.; Miller, W.; Myers, E.W.; Lipman, D.J. Basic local alignment search tool. *J. Mol. Biol.* **1990**, *215*, 403–410. [[CrossRef](#)]
151. Buchfink, B.; Xie, C.; Huson, D.H. Fast and sensitive protein alignment using DIAMOND. *Nat. Methods* **2015**, *12*, 59–60. [[CrossRef](#)] [[PubMed](#)]
152. Mistry, J.; Finn, R.D.; Eddy, S.R.; Bateman, A.; Punta, M. Challenges in homology search: HMMER3 and convergent evolution of coiled-coil regions. *Nucleic Acids Res.* **2013**, *41*, e121. [[CrossRef](#)] [[PubMed](#)]
153. Shimizu, K.; Adachi, J.; Muraoka, Y. ANGLE: A sequencing errors resistant program for predicting protein coding regions in unfinished cDNA. *J. Bioinform. Comput. Biol.* **2006**, *4*, 649–664. [[CrossRef](#)]
154. Hu, H.; Miao, Y.R.; Jia, L.H.; Yu, Q.Y.; Zhang, Q.; Guo, A.Y. AnimalTFDB 3.0: A comprehensive resource for annotation and prediction of animal transcription factors. *Nucleic Acids Res.* **2019**, *47*, D33–D38. [[CrossRef](#)]
155. Thiel, T.; Michalek, W.; Varshney, R.K.; Graner, A. Exploiting EST databases for the development and characterization of gene-derived SSR-markers in barley (*Hordeum vulgare* L.). *Appl. Genet.* **2003**, *106*, 411–422. [[CrossRef](#)]
156. Sun, L.; Luo, H.; Bu, D.; Zhao, G.; Yu, K.; Zhang, C.; Liu, Y.; Chen, R.; Zhao, Y. Utilizing sequence intrinsic composition to classify protein-coding and long non-coding transcripts. *Nucleic Acids Res.* **2013**, *41*, e166. [[CrossRef](#)]
157. Kang, Y.J.; Yang, D.C.; Kong, L.; Hou, M.; Meng, Y.Q.; Wei, L.; Gao, G. CPC2: A fast and accurate coding potential calculator based on sequence intrinsic features. *Nucleic Acids Res.* **2017**, *45*, W12–W16. [[CrossRef](#)]

158. Li, W.; Cowley, A.; Uludag, M.; Gur, T.; McWilliam, H.; Squizzato, S.; Park, Y.M.; Buso, N.; Lopez, R. The EMBL-EBI bioinformatics web and programmatic tools framework. *Nucleic Acids Res.* **2015**, *43*, W580–W584. [[CrossRef](#)]
159. Li, A.; Zhang, J.; Zhou, Z. PLEK: A tool for predicting long non-coding RNAs and messenger RNAs based on an improved k-mer scheme. *BMC Bioinform.* **2014**, *15*, 311. [[CrossRef](#)] [[PubMed](#)]
160. Bray, N.L.; Pimentel, H.; Melsted, P.; Pachter, L. Near-optimal probabilistic RNA-seq quantification. *Nat. Biotechnol.* **2016**, *34*, 525–527. [[CrossRef](#)] [[PubMed](#)]
161. Emms, D.M.; Kelly, S. OrthoFinder: Phylogenetic orthology inference for comparative genomics. *Genome Biol.* **2019**, *20*, 238. [[CrossRef](#)] [[PubMed](#)]
162. Katoh, K.; Standley, D.M. MAFFT multiple sequence alignment software version 7: Improvements in performance and usability. *Mol. Biol. Evol.* **2013**, *30*, 772–780. [[CrossRef](#)]
163. Capella-Gutierrez, S.; Silla-Martinez, J.M.; Gabaldon, T. trimAl: A tool for automated alignment trimming in large-scale phylogenetic analyses. *Bioinformatics* **2009**, *25*, 1972–1973. [[CrossRef](#)]
164. Kalyaanamoorthy, S.; Minh, B.Q.; Wong, T.K.F.; von Haeseler, A.; Jermini, L.S. ModelFinder: Fast model selection for accurate phylogenetic estimates. *Nat. Methods* **2017**, *14*, 587–589. [[CrossRef](#)]
165. Hoang, D.T.; Chernomor, O.; von Haeseler, A.; Minh, B.Q.; Vinh, L.S. UFBoot2: Improving the Ultrafast Bootstrap Approximation. *Mol. Biol. Evol.* **2018**, *35*, 518–522. [[CrossRef](#)]
166. Minh, B.Q.; Schmidt, H.A.; Chernomor, O.; Schrempf, D.; Woodhams, M.D.; von Haeseler, A.; Lanfear, R. IQ-TREE 2: New Models and Efficient Methods for Phylogenetic Inference in the Genomic Era. *Mol. Biol. Evol.* **2020**, *37*, 1530–1534. [[CrossRef](#)]
167. Letunic, I.; Bork, P. Interactive Tree Of Life (iTOL) v5: An online tool for phylogenetic tree display and annotation. *Nucleic Acids Res.* **2021**, *49*, W293–W296. [[CrossRef](#)]
168. Waterhouse, A.M.; Procter, J.B.; Martin, D.M.; Clamp, M.; Barton, G.J. Jalview Version 2—A multiple sequence alignment editor and analysis workbench. *Bioinformatics* **2009**, *25*, 1189–1191. [[CrossRef](#)]